

THE SKULL OF *RAPETOSAURUS KRAUSEI* (SAUROPODA: TITANOSAURIA) FROM THE LATE CRETACEOUS OF MADAGASCAR

KRISTINA CURRY ROGERS¹ and CATHERINE A. FORSTER²

¹Department of Paleontology, Science Museum of Minnesota, 120 W. Kellogg Blvd., St. Paul, Minnesota 55102, krogers@smm.org;

²Department of Anatomical Sciences, Health Sciences Center, Stony Brook University, Stony Brook, New York 11794-8081

ABSTRACT—*Rapetosaurus krausei* (Sauropoda: Titanosauria) from the Upper Cretaceous Maevarano Formation of Madagascar is the best-preserved and most complete titanosaur yet described. The skull of *Rapetosaurus* is particularly significant because most titanosaurs are diagnosed solely on the basis of fragmentary postcranial material, and knowledge of the titanosaur skull has remained incomplete. Material referred to *Rapetosaurus* includes the type skull from an adult that preserves the basicranium, rostrum, mandible, and palate. A second, juvenile skull preserves most of the braincase and cranial vault, as well as some of the palate and lower jaw. Here we provide a detailed description of *Rapetosaurus* cranial anatomy and highlight comparative relationships among known titanosaur and other neosauropod skulls. The *Rapetosaurus* skull is similar to those of diplodocoids in its overall shape, with retracted external nares and an elongated snout. However, extensive tooth distribution and bone articulations surrounding the external narial region and orbit are more similar to those of macronarians like *Camarasaurus* and *Brachiosaurus*. The maxilla, basicranium, paroccipital process, and pterygoid are among the most diagnostic elements of the *Rapetosaurus* skull, along with the enlarged antorbital fenestra, anteroventrally oriented braincase, and mandible. Titanosaur crania exhibit a greater diversity than previously recognized and, in light of *Rapetosaurus*, it is apparent that there is not a narrowly constrained bauplan for the skull of titanosaurs. Broad generalizations about evolution based on previously known, fragmentary fossils require re-evaluation. Ultimately, *Rapetosaurus* will be key in resolving titanosaur higher-level and ingroup phylogeny.

INTRODUCTION

Titanosaurs comprise nearly half of all known sauropod genera, and were the only sauropod lineage to survive to the end of the Cretaceous. Their postcrania are found worldwide, but their skulls are exceptionally rare. Cranial material is known from only ten titanosaurs and is limited to isolated elements and fragmentary braincases (Table 1). In fact, no titanosaur skull found in association with postcrania has ever been fully described or illustrated, and very few instances of direct association of skulls and postcrania have been documented. This nagging lack of association has left even the most basic skeletal morphology of the clade controversial and has precluded detailed study of the higher and lower level phylogeny of the group (e.g., Salgado et al., 1997; Upchurch, 1998; Wilson and Sereno, 1998).

Expeditions to the Maevarano Formation in the Berivotra area of northwestern Madagascar over six field seasons (summaries in Krause et al., 1997, 1999; Rogers et al., 2000) have discovered an astonishingly diverse Late Cretaceous fauna. This fauna includes isolated and associated cranial and postcranial material from two distinct sauropod taxa. Curry Rogers and Forster (2001) named *Rapetosaurus krausei*, the more complete of these two Maevarano Formation titanosaurs, and provided a brief description of its skull and skeleton. *Rapetosaurus* represents the most complete titanosaur yet described, and consists of a nearly complete adult skull and an associated juvenile skull and skeleton. The completeness of the skeleton and, in particular, the presence of a well-preserved skull, has a significant influence on resolution of titanosaur phylogeny (Curry and Forster, 1999a, b; Curry, 2001; Curry Rogers, 2001a, b). Here we provide a detailed description of the skull of *Rapetosaurus krausei* (Fig. 1).

Institutional Abbreviations: **CM**, Carnegie Museum of Natural History, Pittsburgh; **FMNH PR**, Field Museum of Natural History, Chicago; **GSI**, Geological Survey of India; **HMN**,

Humboldt Museum für Naturkunde, Berlin; **ISI**, Indian Statistical Institute, Calcutta; **MACN**, Museo Argentino de Ciencias Naturales, Buenos Aires; **MD-E**, Musée des Dinosauriens, Esperaza; **PIN**, Paleontological Institute, Moscow; **PMU**, Paleontological Museum of Uppsala University, Uppsala; **SMU**, Southern Methodist University, Dallas; **SUNY-SB**, State University of New York at Stony Brook, Stony Brook; **UA**, Université d'Antananarivo, Antananarivo; **UCB**, Université Claude Bernard, Lyon; **ZPAL**, Instytut of Paleobiologii, Polish Academy of Sciences, Warsaw.

GEOLOGY AND BONE ASSOCIATIONS

Like most vertebrate remains found in the Maevarano Formation, all *Rapetosaurus* skull material described herein was recovered from the Campanian-Maastrichtian Anembalemba Member (Rogers et al., 2000). The isolated and partially disarticulated bones of the holotype skull of *Rapetosaurus* (UA 8698) were recovered in 1996 from a single stratum over an area of approximately 1 m² at locality MAD 96-02. Holotype material shows no duplication of elements and exhibits exact sutural articulations. Additional skull material from at least two juvenile sauropods was recovered from another locality, MAD 93-18. Most of these juvenile skull elements were found in close association with a nearly complete juvenile postcranial skeleton. This skeleton was recovered within an area of ~10 m² and also shows no duplication of elements. A number of the juvenile skull elements from MAD 93-18 share autapomorphies with the holotype adult skull of *Rapetosaurus* (Fig. 2), and are thus referred to this taxon and described below (Curry, 2001).

HISTORICAL BACKGROUND AND TAXONOMY

Fragmentary titanosaur remains have been known from Upper Cretaceous strata of Madagascar since Charles Depéret described *Titanosaurus madagascariensis* in 1896 from two pro-

TABLE 1. Titanosaur taxa represented by cranial material. * indicates taxa to which postcranial elements have been attributed. ** indicates taxa directly associated with postcrania.

Taxon	Material	Location	Age
** <i>Ampelosaurus</i>	teeth, dentary, 3 braincases	France	Campanian-Maastrichtian
* <i>Antarctosaurus</i>	1 braincase, dentary	Argentina	Campanian-Maastrichtian
**RH 821 Baja Santa Rosa	2 partial skulls	Argentina	Campanian-Maastrichtian
" <i>Jainosaurus</i> "	3 partial braincases, maxilla, squamosal	India	Campanian-Maastrichtian
Jabalpur indet.	1 partial braincase	India	Campanian-Maastrichtian
** <i>Lirainosaurus</i>	partial basicranium, teeth	Spain	Campanian-Maastrichtian
* <i>Magyarosaurus</i>	partial braincase	Romania	Campanian-Maastrichtian
* <i>Malawisaurus</i>	partial skull, 2 dentaries, teeth	Malawi	Aptian-Albian
<i>Nemegtosaurus</i>	partial skull, dentaries	Mongolia	Campanian-Maastrichtian
<i>Quaesitosaurus</i>	partial skull, dentaries	Mongolia	Campanian-Maastrichtian
** <i>Rapetosaurus</i>	partial juvenile and adult skulls	Madagascar	Campanian-Maastrichtian
** <i>Saltasaurus</i>	1 juvenile braincase	Argentina	Campanian-Maastrichtian
Titanosauria indet.	partial skull	Argentina	Campanian-Maastrichtian

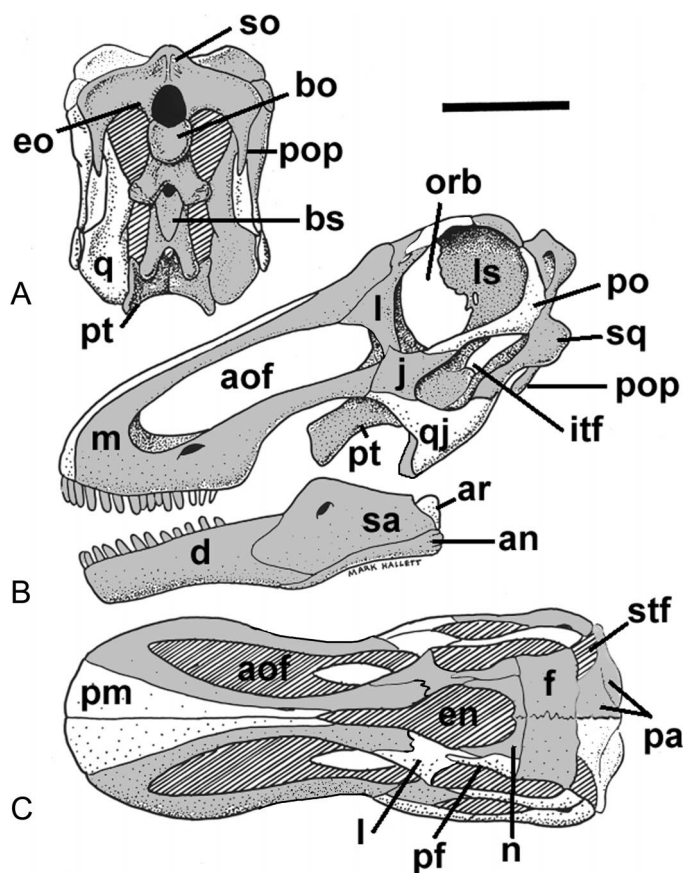


FIGURE 1. *Rapetosaurus krausei* from the Upper Cretaceous Maevarano Formation of Madagascar. This skull reconstruction is a composite based on holotype (UA 8698) and referred specimens (FMNH PR 2184–2192, 2194, 2196–2197) and shown in A, posteroventral view; B, left lateral view; C, dorsal view. Shaded bones are preserved. **Abbreviations:** an, angular; aof, antorbital fenestra; ar, articular; bo, basioccipital; bs, basisphenoid; d, dentary; en, external nares; eo, exoccipital; f, frontal; itf, infratemporal fenestra; j, jugal; l, lacrimal; ls, laterosphenoid-orbitosphenoid; m, maxilla; n, nasal; orb, orbit; pa, parietal; pf, prefrontal; pm, premaxilla; po, postorbital; pop, paroccipital process; pt, pterygoid; q, quadrate; qj, quadratojugal; sa, surangular; so, supraoccipital; sq, squamosal; stf, supratemporal fenestra. Scale bar equals 10 cm.

coelous caudal vertebrae (UCB 92829, 92305), a partial humeral diaphysis (UCB 92831), and a referred large osteoderm (UCB 92827) (Boule, 1896; Depéret, 1896a, b). Presently, we recognize two titanosaur taxa in the Maevarano Formation that are distinguished, in part, by the morphology of their caudal vertebrae (Curry Rogers and Forster, 1999a, b, 2001). Depéret's *T. madagascariensis* syntype includes both morphs of caudal vertebrae, and is therefore considered a nomen dubium (Curry, 2001a, b; Curry Rogers and Forster, 2001). Caudal centrum UCB 92829 corresponds to *Rapetosaurus krausei*. UCB 92829 is thus removed from the syntype of *T. madagascariensis*, and referred to *Rapetosaurus*. The second caudal vertebra in Depéret's syntype, UCB 92305, corresponds to the caudal vertebrae referred to as "Malagasy Taxon B" (Curry 2001; Curry Rogers, 2001a, b, 2002; Curry Rogers and Forster, 2001). This second taxon will be described at a later date.

SYSTEMATIC PALEONTOLOGY

Order SAURISCHIA Seeley, 1888

Suborder SAUROPODA Marsh, 1878

TITANOSAURIA Bonaparte and Coria, 1993

RAPETOSAURUS KRAUSEI Curry Rogers and Forster, 2001

Holotype—UA 8698, adult skull including right maxilla with eight teeth, left maxilla, right lacrimal, left jugal, right and left nasals, right quadrate, right and left pterygoids, partial basioccipital, right paroccipital process, left dentary with 11 teeth, both angulars, right surangular, and five associated teeth (Figs. 1–10, 16–17, 26–32).

Referred Specimens—FMNH PR 2184 right exoccipital/opisthotic, supraoccipital, and laterosphenoid; FMNH PR 2185 right prefrontal, right and left frontals; FMNH PR 2186, right prefrontal; FMNH PR 2187, left surangular; FMNH PR 2188, right parietal; FMNH PR 2189, left squamosal; FMNH PR 2190, right quadrate; FMNH PR 2191, left pterygoid; FMNH PR 2192, right exoccipital-opisthotic; FMNH PR 2194, right angular; FMNH PR 2196, three associated teeth; FMNH PR 2197 fused basioccipital, basisphenoid, parasphenoid; FMNH PR 2209, associated juvenile skeleton; FMNH PR 2210, mid caudal centrum; UCB 92829, mid-caudal centrum (Figs. 1, 11–15, 18–26).

Type Locality and Age—MAD 96-02, Mahajanga Basin, northwestern Madagascar; Anembalemba Member, Maevarano Formation, Upper Cretaceous, Maastrichtian (Rogers et al., 2000).

Diagnosis—See Curry Rogers and Forster (2001) for detailed diagnosis.

DESCRIPTION

The following descriptions include comparisons of *Rapetosaurus* skull morphology with the skulls of other titanosaurs

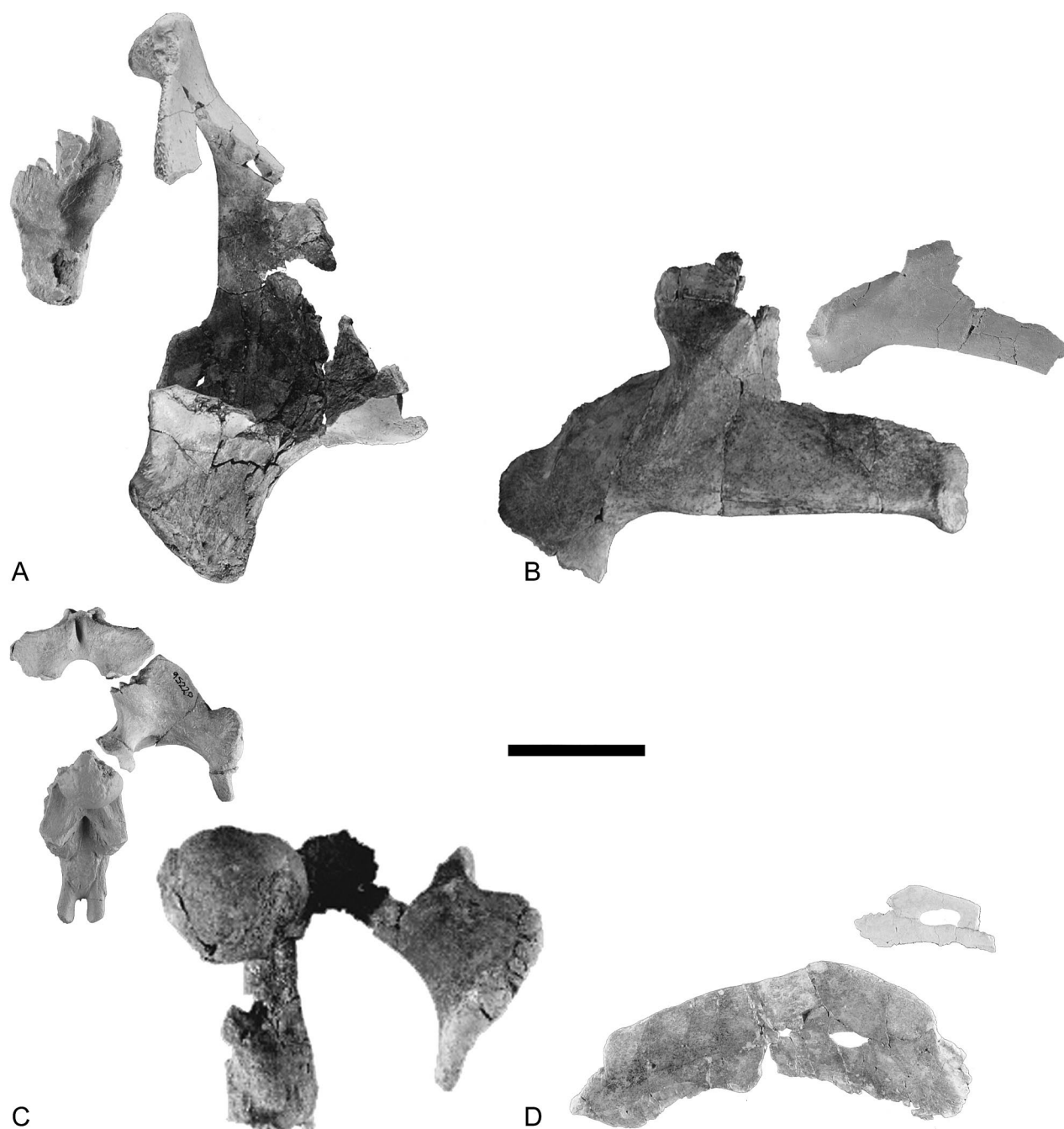


FIGURE 2. *Rapetosaurus krausei* adult and juvenile skull elements compared. **A**, juvenile (FMNH PR 2190) and adult (UA 8698) right quadrates in posterior view; **B**, juvenile (FMNH PR 2191) and adult (UA 8698) left pterygoids in medial view, anterior to right; **C**, adult and juvenile basicrania in posterior view; and **D**, juvenile (FMNH PR 2187) and adult (UA 8698) right surangulars in lateral view. Scale bar equals 3 cm.

and neosauropods. Where possible, key references and specimen numbers are provided. All taxa discussed below (except *Euhelopus*) were personally examined (by KCR) for this study and most comparative data are the direct result of these observations.

Skull

Maxilla—(UA 8698; Figs. 3, 4) Partial left and right maxillae are preserved in the holotype skull. Although neither preserves a complete tooth row, the left maxilla preserves the posterior margin of the caudalmost alveolus. Eight equally spaced

teeth were found in association with the alveolar margin of the right maxilla, although the alveoli themselves were weathered beyond repair. The alveolar margin of the maxilla has space for more than eight teeth, and 12 to 15 teeth may have been present.

The dorsal ascending and jugal (posteroventral) processes are extremely elongate. They arise from the dorsal and posterior borders of the maxillary body, and form the dorsal and ventral margins of an anteriorly enlarged antorbital fenestra. The antorbital fenestra extends anteriorly over at least half the tooth row, a situation unique among sauropods (e.g., Holland, 1924; Wiman, 1929; Janensch, 1935/36; White, 1958; Nowinski,



FIGURE 3. *Rapetosaurus krausei* right maxilla (UA 8698) in **A**, lateral; and **B**, medial views. Scale bar equals 5 cm.

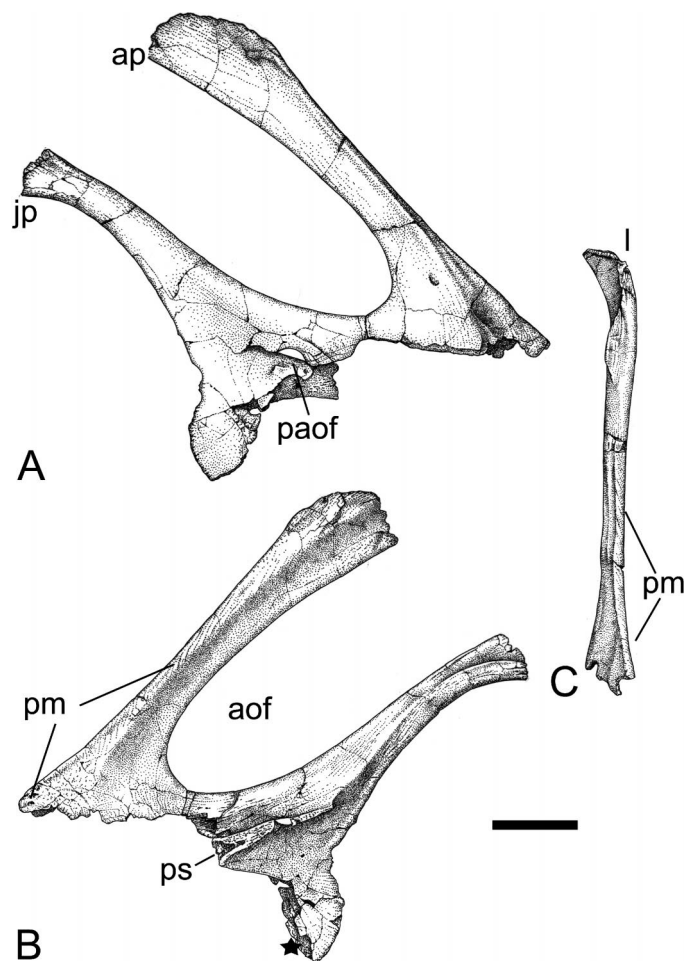


FIGURE 4. *Rapetosaurus krausei* right maxilla (UA 8698) in **A**, lateral view; **B**, medial view; and **C**, anterior view. Star marks posterior-most alveolus. Scale bar equals 5 cm. **Abbreviations:** aof, antorbital fenestra; ap, ascending process; jp, jugal process; paof, preantorbital fenestra; pm, premaxilla facet; ps, palatal shelf.

1971; Berman and McIntosh, 1978; Kurzanov and Bannikov, 1983; Madsen et al., 1995). The antorbital fenestra is bounded posteroventrally by the jugal, and posterodorsally by the lacrimal; the nasal was probably excluded from the fenestra by a maxilla-lacrimal contact. Although there is no sign of any antorbital fossa on the external surfaces of the maxillae, a clearly defined but shallow fossa marks the medial surface of the dorsal ascending and jugal processes. The enlarged antorbital fenestra and narrow jugal process restrict the body of the maxilla to the anterior, alveolar portion. The bodies of both maxillae are incompletely preserved, but each bears a robust, medially directed palatal shelf centered just above the posteriormost alveolus.

Two large, conjoined foramina are situated ventral to the antorbital opening, at the base of the jugal process and just above the palatal shelf (Figs. 3A, 4A). A similarly placed foramen has been described in *Camarasaurus* (White, 1958) as the "posterior alveolar foramen." A large opening, generally termed the preantorbital foramen, is found anterior to the antorbital fenestra and palatal shelf in several other sauropods (e.g., *Apatosau-*

rus, Berman and McIntosh, 1978; *Diplodocus*, Holland, 1924; *Nemegtosaurus*, Nowinski, 1978; Titanosauridae indet., Martinez, 1998). These foramina are thought to transmit neural and vasculature tissue (e.g., "superior alveolar nerve and maxillary artery," White, 1958). Positional data, including placement near the antorbital fenestra, neurovascular grooves emanating from the foramina, and the proximity of these foramina to the palatal shelf, indicate that those observed in *Rapetosaurus* and *Camarasaurus* (e.g., CM11338; Madsen et al., 1995) are homologous to the preantorbital foramen of other sauropods. The posterior placement of this foramen in *Rapetosaurus* may result from the anterior expansion of the antorbital fenestra.

The gracile dorsal ascending process arises from the body of the maxilla anterior to the palatal shelf. The ventral margin of this process is very thin where it forms the dorsal rim of the antorbital fenestra. The process thickens to its dorsal margin and is nearly triangular in cross-section along most of its length. At its distal end, the posterodorsal process expands dorsoventrally and thickens along its ventral margin, where it presumably overlaps the lacrimal (Figs. 3A, 4A). In contrast with *Camarasaurus* (e.g., CM11338; Madsen et al., 1995) and *Euhelopus* (PMU 233, 234; Wiman, 1929), in *Rapetosaurus* the dorsal ascending process lacks any evidence of a medially directed process or shelf forming part of the ventral floor of the nares.

The dorsal ascending process of the maxilla preserves articular surfaces for the premaxilla and the lacrimal (Fig. 4C). Premaxillae are not preserved in any *Rapetosaurus* specimen, but their extensive contact with the maxillae is clearly delimited on the dorsal ascending process. The premaxilla-maxilla contact is marked by a striated anteromedial surface along the proximal two-thirds of the ascending process. This sutural surface is slightly textured and grooved in places, and extends approximately 18 cm along the anterior face of the dorsal ascending process. Distally, this facet is flanked by a lateral neurovascular groove that may represent the position of the subnarial foramen along the premaxilla-maxilla suture, as in other sauropods (e.g., *Brachiosaurus*, HMN t1, s66, s116; *Camarasaurus*, CM 11338; *Diplodocus*, CM 11161, CM 3452; *Euhelopus*, PMU 233, 234; *Nemegtosaurus*, ZPAL MgD-I/9). This neurovascular groove extends ventrally, and terminates where it perforates the maxillary body near the base of the dorsal ascending process via a foramen. The premaxillary articular surface broadly overlaps the anteromedial surface of the maxillary body, but comes to lie on the anterior surface as it approaches the narial opening. Where the premaxillary articulation terminates, the dorsal edge of the dorsal ascending process thickens slightly into a smooth, dorsally facing surface approximately 4 cm long. This smooth surface may represent the ventral margin of the naris.

Behind the narial margin, the dorsal ascending process thickens, curves laterally, and bears an irregular, dorsomedially-facing facet for the lacrimal. Only the anterior portion of this facet is preserved. The anterior end of the lateral process of the nasal may have contacted the dorsal ascending process, but there are no visible facets and neither the nasal nor the maxilla is complete in this region.

The long and dorsoventrally compressed jugal process of the maxilla is a unique feature of *Rapetosaurus*. It arises from the body of the maxilla just posterior to the palatal shelf and results from the extreme dorsoventral constriction of the maxilla posterior to the tooth row. The jugal process is nearly triangular in cross section, bearing a ridge along its medial surface that is confluent with the palatal shelf. Both the dorsal and ventral margins of the jugal process are thin and sharp at the base, but become thicker and blunter distally. The medial surface of the distal jugal process bears a deep V-shaped trough above the medial ridge for reception of the maxillary process of the jugal. A small flange on the maxillary process of the jugal roofs this trough. This “tongue-in-groove” articulation of the maxilla and jugal in *Rapetosaurus* is distinct from the maxillary-jugal connection in other sauropods. In *Brachiosaurus* (HMN t1, s66, s116), *Camarasaurus* (CM 11338), *Diplodocus* (CM 11161), *Euhelopus* (PMU 233, 234), *Nemegtosaurus* (ZPAL MgD-I/9), and *Quaesitosaurus* (PIN 3906/2) the jugal laterally overlaps the deep posterior border of the maxilla via a blunt, dorsoventrally extensive facet.

Although all but the most posterior alveoli in both maxillae are missing, the eight teeth found associated with the right maxilla allow a general interpretation of tooth morphology (described below) and placement. A single, unworn replacement tooth is present in the last alveolus of the right maxilla, confirming that teeth in *Rapetosaurus* were not restricted to the anterior regions of the jaw.

Jugal—(UA 8698; Figs. 5, 6) The jugal has a relatively flat, platelike body with four radiating processes: an anterior maxillary process, a dorsal lacrimal process, a posterodorsal postorbital process, and a ventral quadratojugal process. The jugal is sufficiently well preserved to articulate with the left maxilla and reveal its contributions to the orbit, antorbital fenestra, and infratemporal fenestra (Figs. 1, 5, 6).

The preserved portion of the maxillary process tapers anteriorly but is eroded distally. It shows the beginning of a shallow groove for reception of the medial ridge along the jugal process

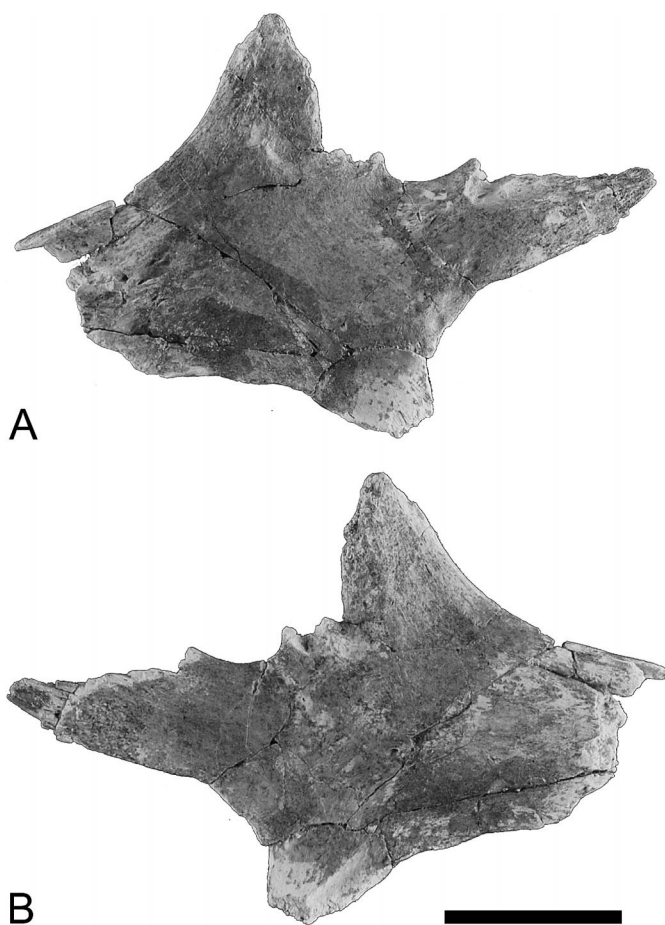


FIGURE 5. *Rapetosaurus krausei* left jugal (UA 8698) in **A**, lateral and **B**, medial views. Scale bar equals 5 cm.

of the maxilla. A small, lateral, horizontally oriented flange roofs this groove. This flange overlaps the small, dorsally facing facet developed on the dorsal edge of the distal jugal process of the maxilla. A ridge is developed on the dorsolateral surface of the jugal maxillary process that fits into the deep groove on the medial surface of the distal jugal process of the maxilla. This mirrored groove-and-ridge structure in the maxilla and jugal locks the elements firmly together.

The robust lacrimal process of the jugal is broadly triangular in lateral view. The lateral surface of the lacrimal process bears a large facet for articulation with the lacrimal. A second, accessory articulation extends along the body of the jugal immediately posterior to this facet. Both facets are slightly depressed and rugose (Figs. 5A, 6A). A faint facet on the lateral surface of the jugal for the distal end of the maxilla meets the lacrimal facet, and implies contact between the maxilla and lacrimal. This contact excludes the jugal from the antorbital fenestra, as in *Nemegtosaurus* (ZPAL MgD-I/9; Nowinski, 1971) and *Quaesitosaurus* (PIN 3906/2; Kurzanov and Bannikov, 1983). The jugal makes a small contribution to the antorbital fenestra in *Brachiosaurus* (e.g., HMN t1, s66, s116; Janensch, 1935/1936). Facets are also present along the entire postero-medial margin of the lacrimal process and on the dorsal margin of the accessory articulation. Thus, the lacrimal broadly overlapped the jugal laterally while simultaneously locking around the posterior and posteromedial margins of the lacrimal process and accessory lacrimal articulation.

A short (2 cm) curved segment of the jugal forms the ventral

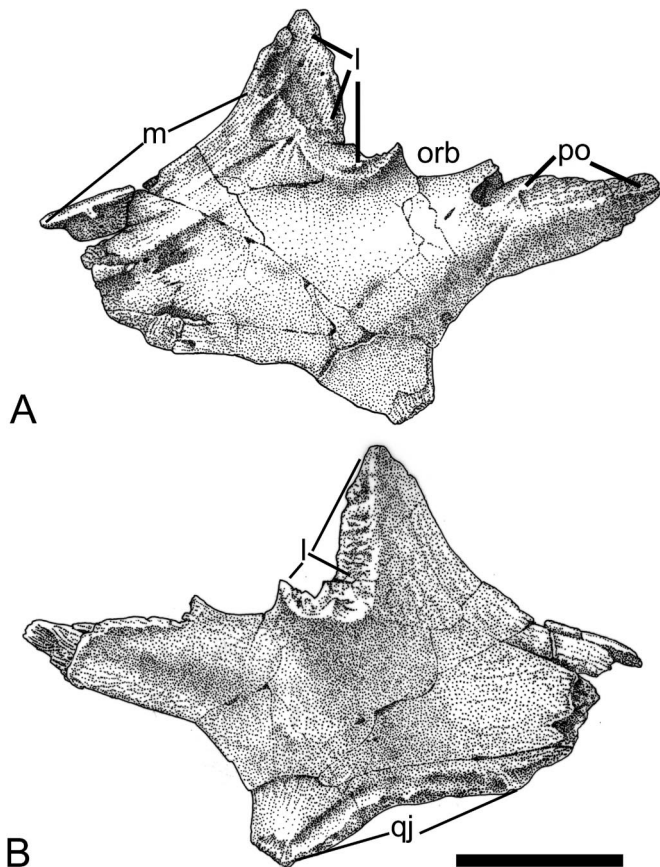


FIGURE 6. *Rapetosaurus krausei* left jugal (UA 8698) in **A**, lateral and **B**, medial views. Scale bar equals 5 cm. **Abbreviations:** **l**, lacrimal facet; **m**, maxilla facet; **orb**, jugal contribution to orbital margin; **po**, postorbital facet; **qj**, quadratojugal facet.

margin of the orbit immediately posterior to the accessory lacrimal articulation. This orbital margin is thin, smooth, and deeply embayed. Projecting posterodorsally is the robust, long, and tapered postorbital process. This process bears a large, deep abutment facet on its dorsolateral surface for the postorbital. The posteroventral edge of the postorbital process forms the thin anteroventral margin of the infratemporal fenestra. The quadratojugal process of the jugal is eroded, as is the area where the postorbital process meets the quadratojugal process. However, on the medial surface of the jugal, a narrow depression extends anteriorly toward the maxillary contact along nearly the entire ventral margin (Figs. 5B, 6B). This depression most likely indicates that the jugal had an extensive overlapping contact with the quadratojugal. The quadratojugal is not preserved, but this long facet indicates that it may have contacted the jugal process of the maxilla, thus eliminating the jugal from the oral margin. Unlike the broad quadratojugal/maxilla contact in *Diplodocus* (e.g., CM 11161; Holland, 1924; Berman and McIntosh, 1978; Yu, 1993), this contact would have been extremely restricted in *Rapetosaurus*.

Lacrimal—(UA 8698; Figs. 7, 8) The lacrimal is triradiate, with an anterior maxillary process, a ventral jugal process, and a dorsal prefrontal process. The elongate, anteroventrally oriented maxillary process arises from the dorsal portion of the lacrimal body. In its anterior two-thirds, the maxillary process bifurcates into dorsal and ventral portions. The ventral portion of the maxillary process bears a distinct groove along its lateral surface, presumably to receive the maxilla's dorsal ascending

process and the anterior process of the prefrontal. Although the dorsal ascending process of the maxilla is poorly preserved, a corresponding hollow on its medial surface supports this interpretation. The ventral margin of the lacrimal's maxillary process is slightly embayed and confluent with the lacrimal body and jugal process, where it forms the posterodorsal border of the antorbital fenestra. The dorsal portion of the maxillary process forms a smooth, medially curved shelf that is slightly elevated from the rest of the lacrimal and forms the lacrimal contribution to the external narial opening (Figs. 1C, 7B, 8B). The smooth narial shelf occupies the dorsal margin of the lacrimal and continues posterodorsally onto the dorsomedial surface of the prefrontal process (see below). The lacrimal also contributes to the external naris in *Nemegtosaurus* (ZPAL MgD-I/9; Nowinski, 1971). Lacrimals in both taxa bear anterior processes that are overlapped laterally by the prefrontal, and medially by the lateral nasal process. The general morphology of the *Rapetosaurus* lacrimal is "L-shaped," as in diplodocoids (e.g., *Diplodocus* CM 11161), but is far more robust than in any other sauropod. However, the articulations between lacrimal, nasal, and prefrontal differ from those bounding the external nares in *Diplodocus* (e.g., CM 11161; Berman and McIntosh, 1978; Yu, 1993). In all described diplodocoids (e.g., *Diplodocus* Holland, 1924; *Dicraeosaurus* Janensch, 1935/1936), the lacrimal is excluded from the narial margin by the nasal/prefrontal contact. In *Brachiosaurus* (e.g., HMN t1, s66, s116; Janensch, 1935/1936) and *Camarasaurus* (e.g., CM 111338; Madsen et al., 1995), the narial opening is bound by only the nasal, premaxilla, and maxilla. In *Nemegtosaurus* (ZPAL MgD-I/9; Nowinski, 1971) and *Rapetosaurus* the lacrimal contributes to the narial margin. The lacrimal is unknown for all other titanosaurs.

The prefrontal process of the lacrimal is broken distally. In lateral view, a distinctive groove sweeps along its lateral face and is continuous with the lateral groove for reception of the dorsal ascending process of the maxilla. A sharp, obliquely oriented ridge bounds the groove posteriorly, and marks the lacrimal's articulation with the anterior process of the prefrontal. The prefrontal was completely excluded from the external narial opening and from articulation with the maxilla by the intermediate position of the lacrimal. Just as in *Nemegtosaurus* (ZPAL MgD-I/9; Nowinski, 1971), the prefrontal lies lateral to the lacrimal.

The jugal process of the lacrimal extends ventrally from the body of the lacrimal to broadly contact the jugal. The proximal portion of the jugal process is nearly triangular in cross-section; it is narrow anteriorly where it forms the posterior margin of the antorbital fenestra, and thicker posteriorly where it bounds the orbit. In lateral view, the jugal process remains robust throughout its length. A deep, rugose slot divides the distal jugal process into medial and lateral portions. The lateral plate of the bifurcated jugal process is broader than the medial plate and completely overlaps the entire lateral surface of the lacrimal process of the jugal. The medial plate fits over the posteromedial margin of that process. This results in a tightly locked lacrimal-jugal articulation. The medial surface of the jugal process is marked by a dorsoventrally elongate prominence that extends up to the base of the prefrontal process. This prominence is narrow and slightly rugose distally, but becomes anteroposteriorly expanded and broadly flattened dorsally. The prominence is broken, but presumably formed the medial side of the lacrimal foramen at the orbit.

The body of the lacrimal is broader anteroposteriorly than transversely. The lacrimal foramen opens just below the prefrontal articulation. The suboval lacrimal foramen opens onto the posterolateral surface, immediately anterior to the orbital margin. As in *Nemegtosaurus* (ZPAL MgD-I/9; Nowinski,

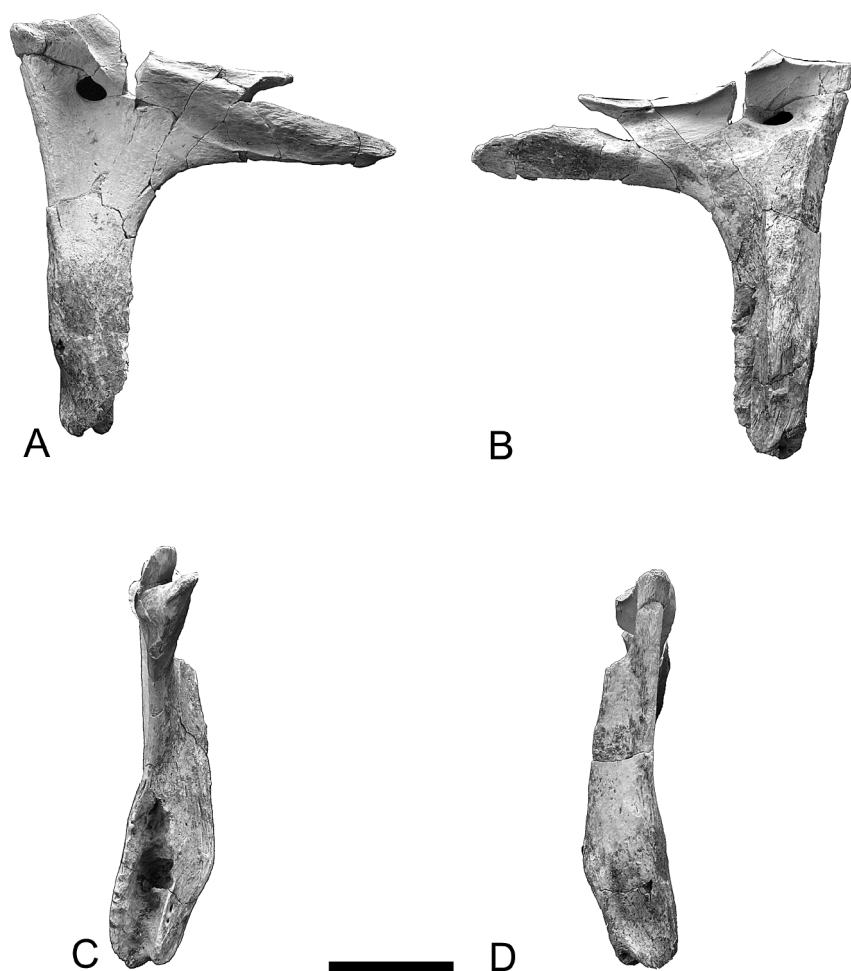


FIGURE 7. *Rapetosaurus krausei* right lacrimal (UA 8698) in **A**, lateral view; **B**, medial view; **C**, anterior view; and **D**, posterior view. Scale bar equals 5 cm.

1971), the lacrimal foramen perforates the lacrimal body in lateral view.

Nasal—(UA 8698; Figs. 9, 10) Partial left and right nasals preserved with the holotype indicate that the nasals are retracted and have a relatively restricted extent in *Rapetosaurus*. The body of the nasal is dorsoventrally compressed, gently arched from side to side, and is anteroposteriorly shortened. Its lateral margin is deeply embayed and bears a well-developed facet for the prefrontal (Figs. 9F, 10C). Neither specimen preserves the contact surface for the contralateral nasal.

The preserved posterior margin of the nasal is slightly concave and thin where it overlaps the frontal. A shallow, triangular depression occurs on the ventral surface of the nasal where it overlaps the frontal and abuts the prefrontal. The nasals have a broadly arching lateral process that does not curve medially. This broader curvature indicates that the posterior narial border was similarly broad. Anteriorly, the nasal has a slender, tapering lateral process that may meet the dorsal ascending process of the maxilla. The lateral nasal process is incomplete in both specimens, but the preserved maxilla and lacrimal both bear smooth margins that may represent their contributions to the rim of the external naris. The medial surface of the lateral nasal process is broadly rounded; this margin becomes thinner and sharper along the anterior margin of the nasal body. Along with the laterally curving dorsal ascending process of the maxilla, the nasals indicate narial retraction, but not as far posteri-

orly as observed in diplodocoids (e.g., *Diplodocus*, CM 11161; Berman and McIntosh, 1978; Yu, 1993). In *Rapetosaurus*, the posterior margin of the external nares lies posterior to the anterior margin of the orbit, but the narial opening appears to extend far anteriorly, dorsal to the antorbital fenestrae (Fig. 1B, C).

The anterior margin of the nearly complete left nasal body is nearly straight and shows no signs of either an embayment or a long, median premaxillary process. The preserved nasal morphology of *Rapetosaurus* suggests that the nasals had a relatively reduced and blunt premaxillary process. This is in contrast with *Camarasaurus* (e.g., CM 11338; Madsen et al., 1995) and *Brachiosaurus* (e.g., HMN t1, s66, s116; Janensch, 1935/1936), which show robust, long premaxillary processes. This interpretation of nasal morphology suggests that *Rapetosaurus* had undivided, retracted external nares similar to that of *Diplodocus* and *Nemegtosaurus*, and different from most macronarians. Witmer (2001) recently reinterpreted the position of the fleshy nostrils in sauropods and other dinosaurs with retracted bony external nares. In contrast with the view that the caudally retracted naris in taxa like *Diplodocus* indicated the full extent of the narial fossa, Witmer outlined an argument for the anterior extension of this fossa on the basis of osteological correlates of vasculature and other narial soft tissues. The result is a rostral positioning of the fleshy nostril in *Diplodocus*. Since the premaxilla is not preserved in *Rapetosaurus*, this hypothesis is

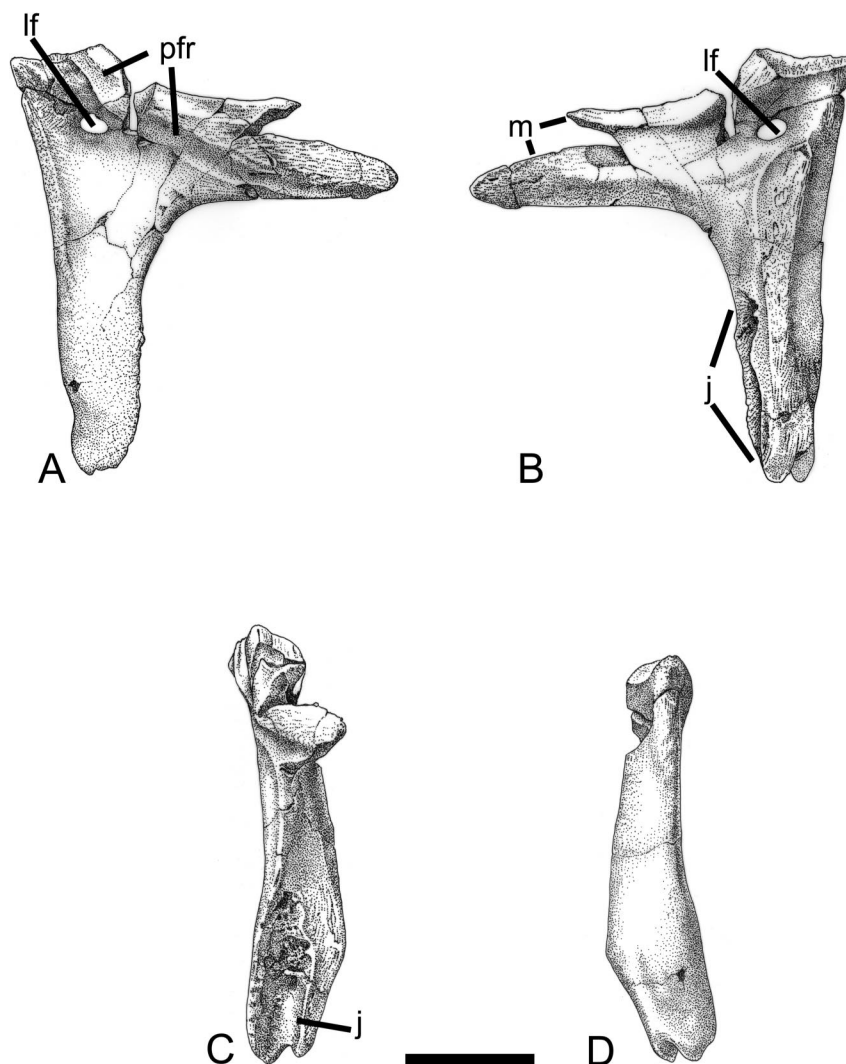


FIGURE 8. *Rapetosaurus krausei* right lacrimal (UA 8698) in **A**, lateral view; **B**, medial view; **C**, anterior view; and **D**, posterior view. Scale bar equals 5 cm. **Abbreviations:** **l**, lacrimal articulation with jugal; **lf**, lacrimal foramen; **m**, lacrimal articulation with maxilla; **pfr**, lacrimal articulation with prefrontal.

impossible to test. However, the articulation of the nasals and maxillae do indicate the presence of a rostrally-expanded narial fossa similar to that observed in *Diplodocus*. Thus, it is likely that the fleshy nostril in *Rapetosaurus* was also rostrally positioned.

Prefrontal—(FMNH PR 2185, FMNH PR 2186; Figs. 11, 12) Two right prefrontals were recovered from MAD 93-18. FMNH PR 2185 articulates precisely with a well preserved right frontal (FMNH PR 2185). Although the prefrontals described here are associated with juvenile cranial and postcranial material, their sutural surfaces match those on the adult nasal and lacrimal.

The prefrontal is sigmoid in shape in both dorsal and lateral views (Figs. 11A, D, 12A, D). In lateral view, the ventral margin of the posterior two-thirds of the prefrontal is concave where it forms part of the anterodorsal orbital margin. The orbital margin of the prefrontal is thickly rounded and slightly rugose; these rugosities are more pronounced posteriorly. The anterior orbital margin of the prefrontal terminates in a small, distinct, ventrolaterally directed facet for the lacrimal. This facet fits into a groove on the body of the lacrimal and is thus overlapped, in part, by the lacrimal. A short, tapered process

extends anterior to this lacrimal facet and overlaps the lateral surface of the dorsal margin of the lacrimal. It may extend anteriorly to contact the posterodorsal process of the maxilla. This contact cannot be confirmed due to erosion of both elements. A small neurovascular foramen pierces the anterior process of the prefrontal immediately in front of the lacrimal facet. The moderately elongate, gracile prefrontal body contrasts with the short, blocky prefrontal bodies observed in some sauropods (e.g., *Brachiosaurus* HMN t1, s66, s116; Janensch, 1935/1936; *Camarasaurus* CM 11338; Madsen et al., 1995). However, elongate, tapered anterior processes are common even among taxa such as *Brachiosaurus* (e.g., HMN t1), which have more robust prefrontal bodies.

The posterior portion of the prefrontal is transversely expanded to form a moderately extensive prefrontal contribution to the roof of the orbit. Its irregular posterior margin is transversely oriented and overlaps slightly less than half of the anterior margin of the frontal. A deep, narrow facet on the ventrolateral surface of this margin accommodates a shallow facet on the dorsal surface of the frontal. Posteromedially, the prefrontal forms an acute angle that broadly overlaps the frontal. A similar condition is present in *Apatosaurus* (Berman and Mc-



FIGURE 9. *Rapetosaurus krausei* nasal (UA 8698). **A**, right nasal in dorsal view; **B**, right nasal in ventral view; **C**, left nasal in dorsal view; **D**, left nasal in ventral view; **E**, right nasal in medial view; and **F**, right nasal in lateral view. Scale bar equals 3 cm.

Intosh, 1978), *Diplodocus* (Holland, 1924; Berman and McIntosh, 1978; Yu, 1993), and *Euhelopus* (Wiman, 1929), and may also be common among titanosaurs (e.g., *Antarctosaurus*, MACN 6804; Huene, 1929; *Saltasaurus*, PVL 4017/162; Powell, 1992).

In dorsal view, the prefrontal narrows anterior to the frontal contact, and curves, first laterally then medially. The nasal articular facet dominates the dorsomedial surface of the prefrontal. A small ridge extends forward on the dorsal surface of the prefrontal marking the margin of the nasal contact (Figs. 11C, 12C). This ridge begins at the element's posterior margin, becomes more prominent anterolaterally, and reaches the lateral margin of the prefrontal at the lacrimal facet. The portion of the prefrontal medial to this ridge faces dorsomedially and

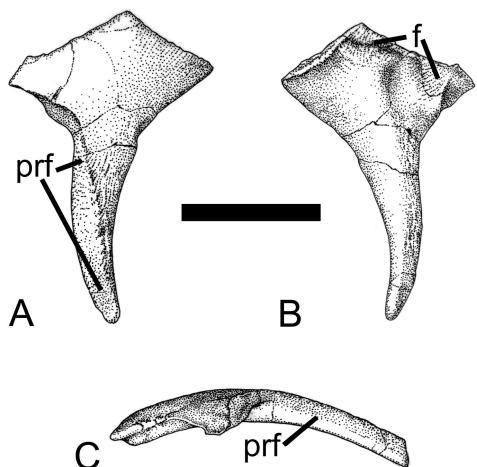


FIGURE 10. *Rapetosaurus krausei* right nasal (UA 8698) in **A**, dorsal view with anterior end down; **B**, ventral view; and **C**, lateral view. Scale bar equals 3 cm. **Abbreviations:** f, frontal facet; prf, prefrontal facet.

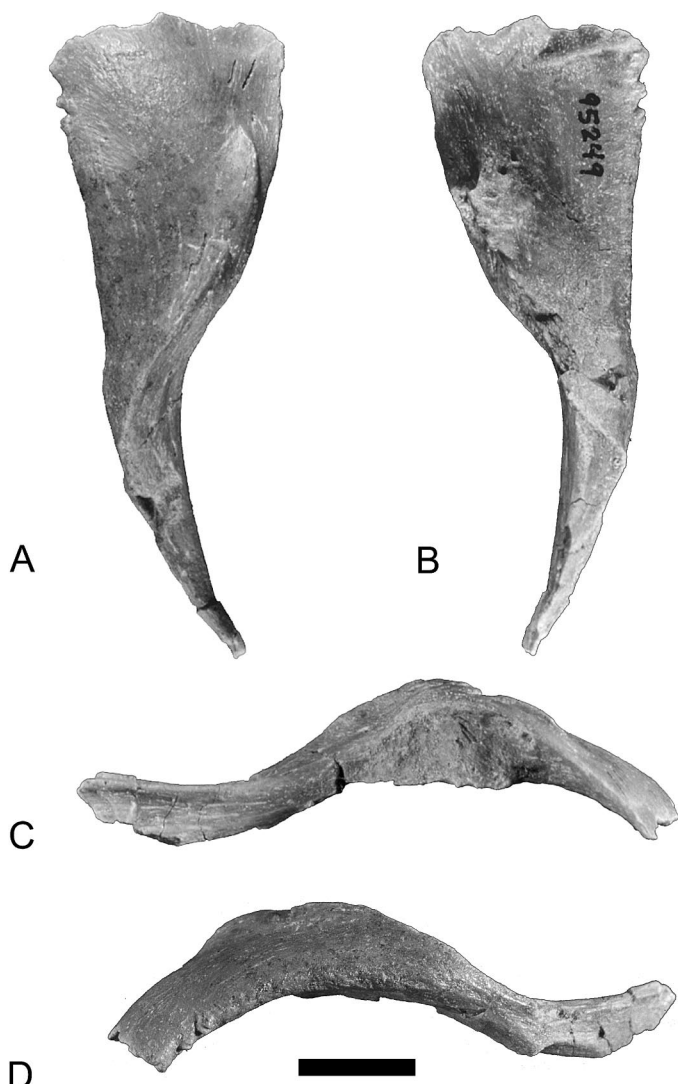


FIGURE 11. *Rapetosaurus krausei* right prefrontal (FMNH PR 2185) in **A**, dorsal view with anterior end down; **B**, ventral view with anterior end down; **C**, medial view with anterior end left; and **D**, lateral view with anterior end right. Scale bar equals 1 cm.

forms the articular surface for the nasal. This articular surface is broadest along the center of the prefrontal, and narrows anteriorly and posteriorly. A deep, nearly vertical concavity lies ventral to the posterior half of the prefrontal-nasal suture, and is separated from it by a bony ridge that forms the ventral margin of the suture. This ridge is confluent with a second ridge on the underside of the prefrontal. Thus, the concavity on the ventromedial surface of the prefrontal is confluent with the broad V-shaped frontal surface that roofs the exit for the olfactory nerve (CN I).

Frontal—(FMNH PR 2185; Fig. 13) Left and right frontals articulate precisely with each other via a deeply interdigitating median suture. The articulated frontals form a subrectangular plate that is wider transversely than anteroposteriorly, as in other sauropods. Dorsomedial convexities on each frontal result from a distinctive doming of the cranial cavity. This dome occupies approximately the medial two-fifths of each frontal, as in *Ampelosaurus* (MD-E C3-761), *Antarctosaurus* (MACN 6804; Huene, 1929), *Saltasaurus* (PVL 4017/162; Powell, 1986, 1992) and in an undescribed titanosaur from the

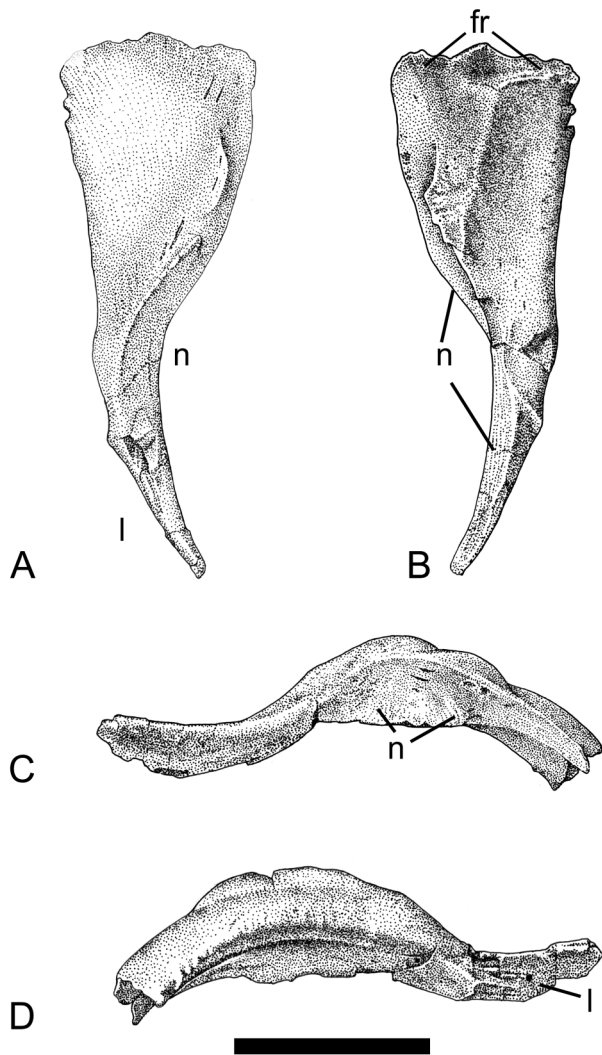


FIGURE 12. *Rapetosaurus krausei* right prefrontal (FMNH PR 2185) in **A**, dorsal view with anterior end down; **B**, ventral view with anterior end down; **C**, medial view with anterior end left; and **D**, lateral view with anterior end right. Scale bar equals 1 cm. **Abbreviations:** f, frontal facet; n, nasal facet; l, lacrimal facet.

Baja Santa Rosa Formation of Argentina (MACN RH821), and an unnamed specimen from the Lameta Formation of Jabalpur, India (ISI R162; Chatterjee and Rudra, 1996). Lateral to the cranial cavity, the frontal flares slightly dorsally as it forms the broad roof of the orbital cavity. The cranial cavity and orbital roof are separated on the underside of the frontal by a thick, interdigitating suture that receives the fused laterosphenoid/orbitosphenoid. In lateral view, the orbital roof is gently arched from front to back and transversely concave. The orbital margin is ornamented with fairly regular, tooth-like rugosities that are more prominent posteriorly. The dorsal margin of a large supraorbital foramen incises the posterior portion of the orbital margin.

The orbital roof is separated from the nasal cavity on the ventral surface of the frontal by a strong ridge that extends anterolaterally from the frontal-orbitosphenoid suture. This ridge is confluent with a similar structure on the underside of the prefrontal and separates the orbital roof from the CN I exit. The anterior margin of the frontal is dorsoventrally compressed where it articulates with the prefrontal and nasal, and ventrally

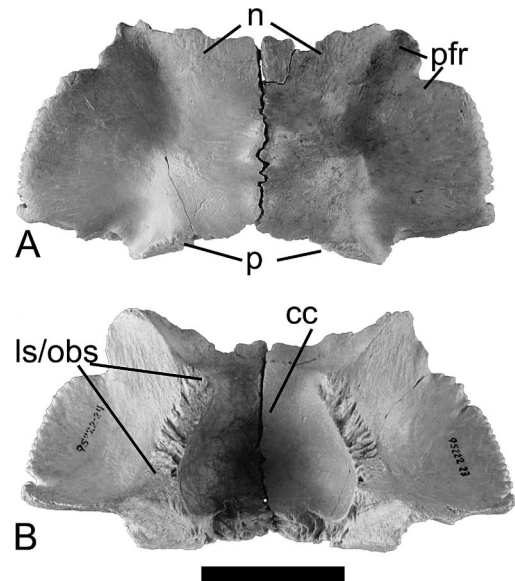


FIGURE 13. *Rapetosaurus krausei* articulated right and left frontals (FMNH PR 2185), anterior end facing up in **A**, dorsal view; and **B**, ventral view. Scale bar equals 3 cm. **Abbreviations:** cc, cranial cavity; ls/obs, laterosphenoid/orbitosphenoid suture; n, nasal facet; p, parietal facet; pfr, prefrontal facet.

depressed relative to the orbital margin. A deep lateral notch in the anterior frontal allows the prefrontal greater access to the orbital margin. Medial to this notch, the anterior margin of the frontal bears a faint, depressed transverse facet that receives part of the prefrontal (laterally) and nasal (medially). The nasal occupies slightly more than half of the anterior width of the frontal; the prefrontal slightly less than half.

Posteriorly, the frontal contacts the parietal via an oblique (anteromedial-posterolateral) suture. This highly interdigitating suture faces both posteriorly and ventrally so that the frontal sits both on and in front of the parietal. This suture occupies the medial three-fifths of the posterior frontal margin. The ventral surface of the posterolateral frontal forms an oval facet that articulates with a corresponding facet on the laterosphenoid. There is an extensive facet for the postorbital on the posterolateral two-fifths of the frontal.

Parietal—(FMNH PR 2188; Figs. 14, 15) The right parietal recovered from MAD 93–18 does not articulate with the right frontal and appears to be from a slightly larger individual. However, examination of the sutures on both elements reveals a match in orientation and morphology. This parietal is thus referred to *Rapetosaurus*.

The parietal is greatly compressed anteroposteriorly ($\leq 1/2$ maximum length of frontal) as in other sauropods (e.g., *Camarasaurus*, CM 11338; Madsen et al., 1995; *Diplodocus*, CM 11161; Yu, 1993; *Nemegtosaurus*, ZPAL MgD-I/9; Nowinski, 1971), and bears a short, straight, interdigitating midline suture. Anteriorly, the parietal meets the frontal along a complex suture that is deeper along its lateral aspect. This lateral portion of the frontal suture bears a cup-like dorsal depression so that the frontal sits both on and in front of the parietal along the lateral portion of their suture. The postorbital likely articulated with the lateralmost portion of this cup-like suture. However, this is impossible to confirm due to the absence of a postorbital in any of the skulls and the lack of articulation between the preserved frontal and parietal. On the ventral surface of the parietal, immediately beneath the cup-like suture, is a large, flat facet that

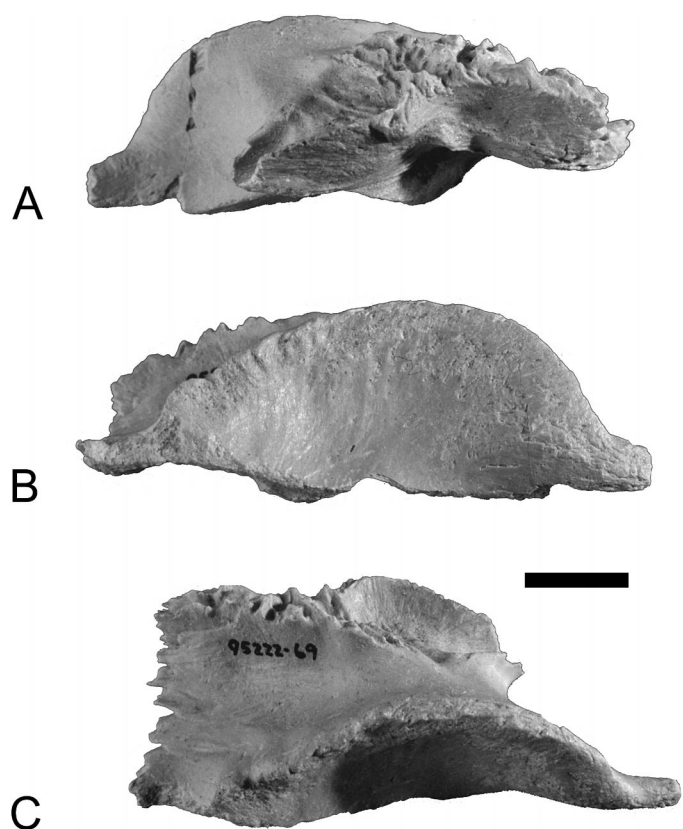


FIGURE 14. *Rapetosaurus krausei* right parietal (FMNH PR 2188) in **A**, anterior view; **B**, posterior view; and **C**, dorsal view with anterior end up. Scale bar equals 1 cm.

meets part of the crista antotica of the laterosphenoid (Fig. 15D).

The parietal extends laterally behind its contact with the frontal to form a laterally tapering squamosal process. The lateral margin of the parietal is thus oriented nearly transversely for most of its length. The anterior margin of this process is smooth and forms the posterior and medial portion of the upper temporal opening. The distal end and ventral portion of the squamosal process is eroded.

When viewed posteriorly (Fig. 15B), the parietal is dorsoventrally deep and exhibits a gently concave face that is inclined slightly anteriorly. The dorsal margin of this face is highly arched. It is approximately 2 cm high at its midpoint and thins both medially (toward the midline) and laterally (along the squamosal process) to less than 0.5 cm (although the ventral border of this process is abraded). The dorsal margin of the arched posterior face is moderately rugose. Centered on the ventral surface of the posterior face is a large, ellipsoidal facet for the exoccipital (laterally) and supraoccipital (medially). The posteromedial corner of the parietal is eroded and missing. The dorsal surface of the parietal between the frontal suture and posterior face is deeply concave.

The parietals of *Brachiosaurus* (e.g., HMN t1, s66, s116; Janensch, 1935/1936) and *Rapetosaurus* are similarly antero-posteriorly expanded centrally, and tapered laterally. However, in a conformation more similar to diplodocoids (e.g., *Dicraeosaurus*, HMN dd307; Janensch, 1935/1936), the articulated parietals and frontals form a shallow median depression on the skull roof. The anterior canting of the posterior parietal face is known to occur in most other purported titanosaurs (i.e., an as yet unidentified titanosaur from Jabalpur, India, ISI R162; Chat-

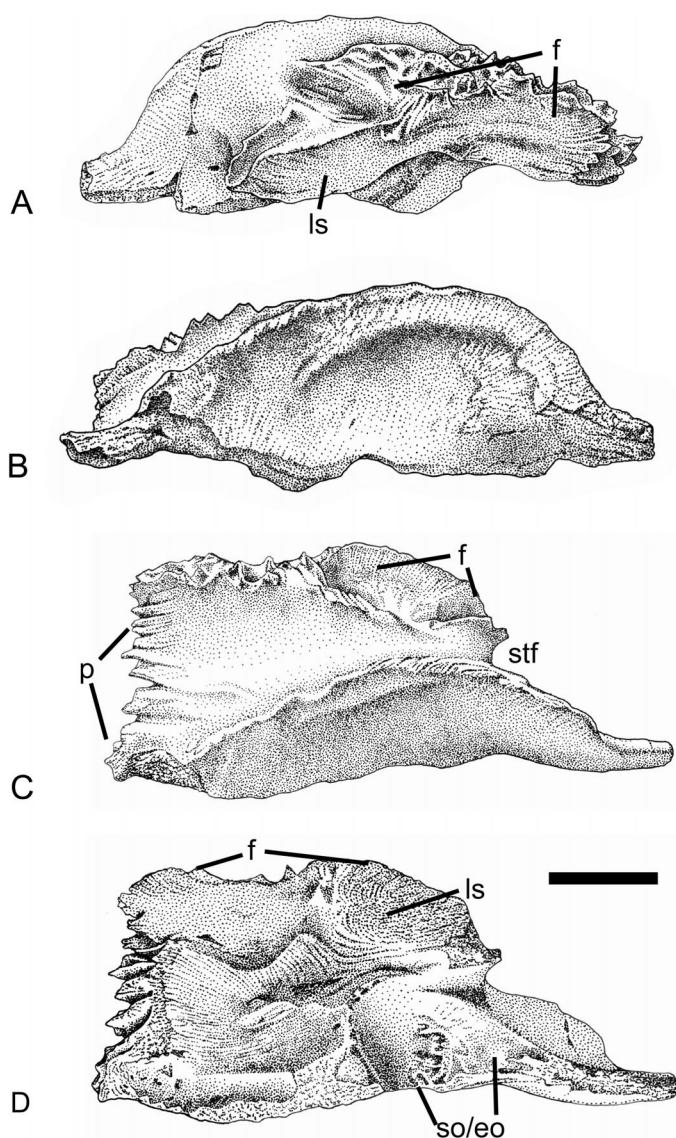


FIGURE 15. *Rapetosaurus krausei* right parietal (FMNH PR 2188) in **A**, anterior view; **B**, posterior view; **C**, dorsal view with anterior end up; and **D**, ventral view with anterior end up. Scale bar equals 1 cm. **Abbreviations:** f, frontal facet; ls, laterosphenoid facet; p, parietal facet; so/eo, supraoccipital/exoccipital facet; stf, supratemporal fenestra.

terjee and Rudra, 1996; *Antarctosaurus wichmannianus*, MACN 6804; Huene, 1929; *Nemegtosaurus*, ZPAL MgD-I/9; Nowinski, 1971; *Quaesitosaurus*, PIN 3906/2; Kurzanov and Bannikov, 1983; *Malawisaurus*, SMU MAL 202-2, 3; *Saltausaurus*, PVL 4017/161; Powell, 1992; *Jainosaurus*, ISI R199; Berman and Jain, 1983; GSI K27/497; Huene and Matley, 1932). An elongate lateral parietal process is also pervasive among titanosaurs, with the exception of *Quaesitosaurus* (PIN 3906/2; Kurzanov and Bannikov, 1983).

Quadrate—(UA 8698, FMNH PR 2190; Figs. 2, 16, 17) The right quadrate of the holotype is nearly complete, and includes the head, posterior shaft, partial pterygoid wing, and the articular condyle. A juvenile right quadrate (FMNH PR 2190) preserves only the articular surface and a portion of the pterygoid process.

The quadrate of *Rapetosaurus* is unusual in a number of aspects. In most sauropods (e.g., *Brachiosaurus*, HMN t1, s66, s116; Janensch, 1935/1936; *Camarasaurus*, CM 11338; Mad-

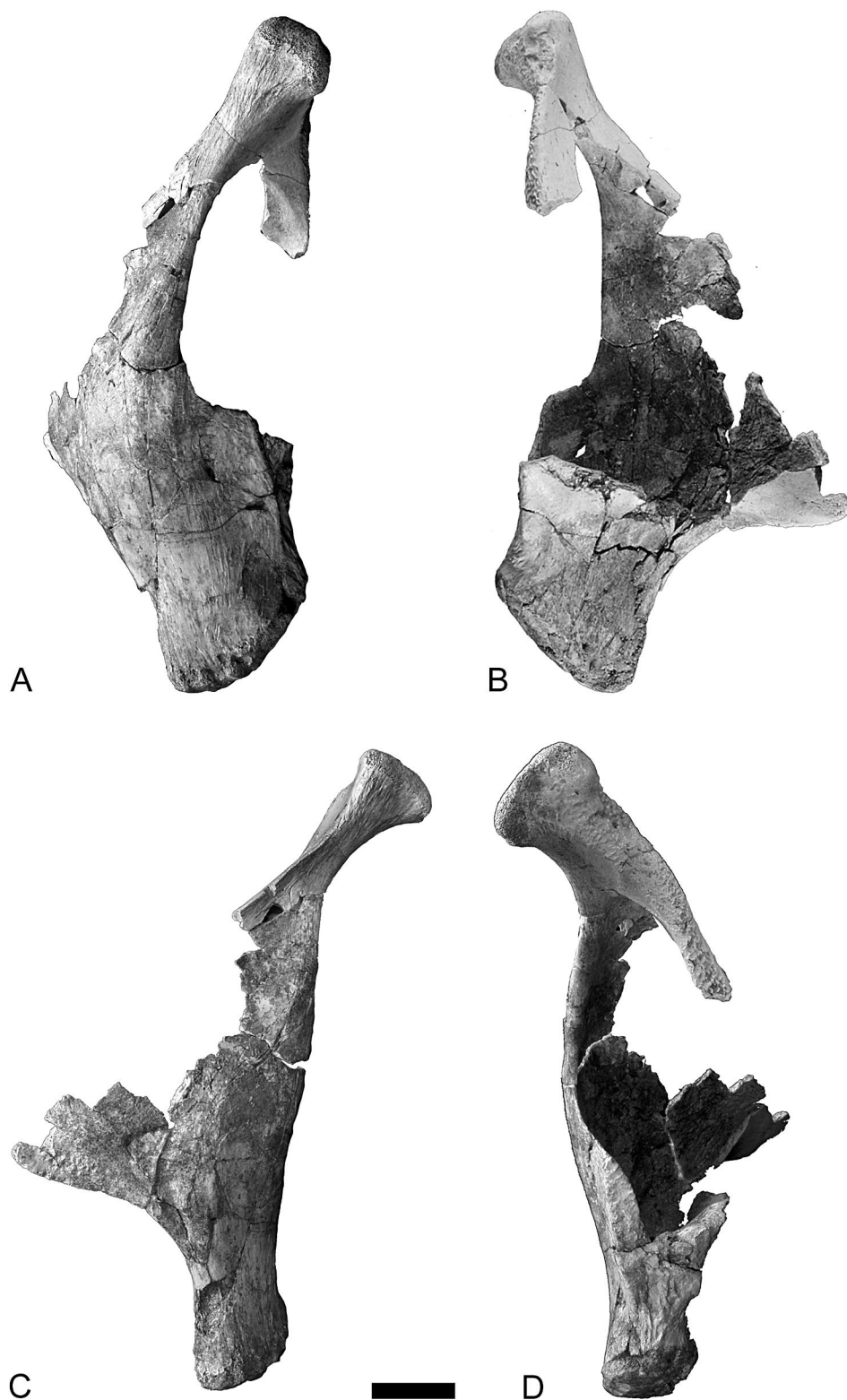


FIGURE 16. *Rapetosaurus krausei* right quadrate (UA 8698) in **A**, anterior view with dorsal end up; **B**, posterior view with dorsal end up; **C**, medial view with dorsal end up; and **D**, lateral view with dorsal end up. Scale bar equals 3 cm.

sen et al., 1995; *Diplodocus*, CM 11161; Berman and McIntosh, 1978) the quadrate shaft is thick and robust with a vertically oriented depression or “trough” along its posterior margin. However, in *Rapetosaurus* the quadrate shaft and, to some ex-

tent, the pterygoid wing of the quadrate are extremely inflated and indented by a cavernous hollow space that opens along most of its posterior surface. This results in the quadrate shaft being reduced to thin plates of bone lying medial and lateral to

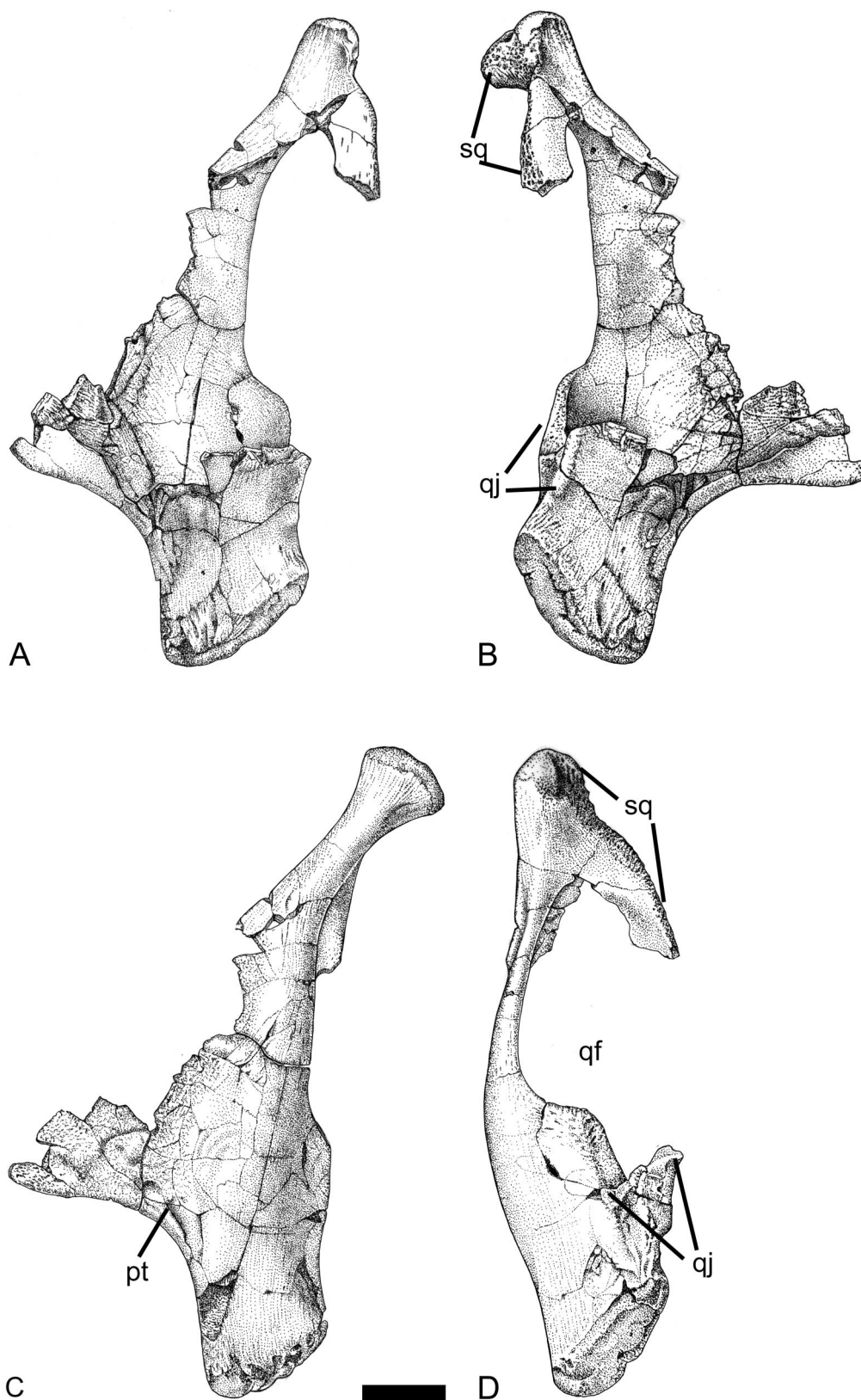


FIGURE 17. *Rapetosaurus krausei* right quadrate (UA 8698) in **A**, anterior view with dorsal end up; **B**, posterior view with dorsal end up; **C**, medial view with dorsal end up; and **D**, lateral view with dorsal end up. Scale bar equals 3 cm. **Abbreviations:** **pt**, pterygoid facet; **qf**, posterolateral quadrate fossa; **qj**, quadratojugal facet; **sq**, squamosal facet.

the hollow space. These plates converge anteriorly to form the anterior portion of the pterygoid wing, ventrally to form the articular condyle, and dorsally to form the condylar head. The medial plate is nearly complete in the holotype, while the distal half of the lateral plate is present in FMNH PR 2190. A comparable quadrate is also found in *Malawisaurus* (SMU MAL 203; Gomani, 1998), *Quaesitosaurus* (PIN 3906/2; Kurzanov and Bannikov, 1983), and an as yet undescribed Argentine titanosaur (Martinez, 1998). The quadrates of *Nemegtosaurus* (ZPAL MgD-I/9) are insufficiently preserved to determine the extent of quadrate excavation.

The quadrate head is sharply bent posteriorly relative to the quadrate shaft (Fig. 17C). In proximal view the quadrate head is subtriangular, with a rounded, posteriorly directed apex. The proximal, posterior, medial, anterior, and anterolateral surfaces of the quadrate head are smooth and form the ball of the squamosal-quadrate articulation. However, the posterolateral side of the quadrate head is deeply rugose; this texture continues down the lateral plate of the quadrate shaft, presumably representing the contact surface for the ventral process of the squamosal. Although the lateral plate is broken at this point in UA 8698, the preserved distal portion of the lateral plate in FMNH PR 2190 also bears rugose pits, suggesting that this facet for the squamosal articulation was extensive and continuous for at least two-thirds the length of the quadrate. This deep, rugose suture and the extensive overlap of the squamosal on the quadrate imply tight articulation of these two elements.

A rugose, V-shaped scar for the quadratojugal is present on the distolateral surface of the quadrate (Figs. 16C, 17C). It extends proximally a short distance on both the lateral and medial plates of the shaft, and distally to the articulation. The scars for the quadratojugal and squamosal appear to be confluent, indicating that the entire lateral surface of the quadrate was probably covered by the squamosal and quadratojugal. The medial plate of the shaft is deeply embayed proximal to the quadratojugal scar.

The large pterygoid wing of the quadrate is anteroposteriorly expansive. The distal end of the medial surface bears two facets for reception of the quadrate process of the pterygoid. The dorsal facet is broad and weakly defined, whereas the ventral facet is more deeply excavated and narrow. This morphology contrasts dramatically with the simple, unexpanded pterygoid wing of the *Malawisaurus* quadrate (SMU MAL 203, Gomani, 1998).

Squamosal—(FMNH PR 2189; Fig. 18) The squamosal consists of a stout body that contacts the postorbital, parietal, and exoccipital, and a long, slender ventral process overlaps the lateral surface of the quadrate. The posterior three-fourths of the medial surface of the squamosal body bears a large, deep scar for reception of the paroccipital process. The posterior portion of this scar is concave with a sharp dorsal rim. The anteromedial one-fourth of the squamosal body is dorsoventrally compressed and likely received the squamosal process of the parietal. In lateral view, the anterior margin of the squamosal body is embayed and bears a blunt, rounded edge that forms a small portion of the posterior margin of the supratemporal fenestra. Immediately ventrolateral is a deep embayment for reception of the postorbital. A deep concavity, confluent with the supratemporal fenestra, excavates the medial and anteroventral body of the squamosal, and extends medial to the postorbital articulation (Fig. 18B). The squamosal lacks the prominent medial process characteristic of *Diplodocus* (e.g., CM 11161, CM 3452; Yu, 1993).

The ventral process extends from the posterior body of the squamosal. In lateral view the ventral process is bowed forward, reflecting the identical curve of the quadrate shaft. It is straight in anterior view. The ventral process flares and thins toward its distal end, which is damaged and incomplete. The lateral surface of the ventral process is gently convex; the me-

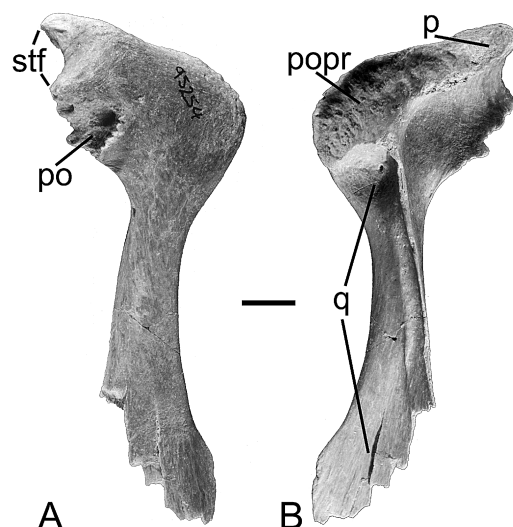


FIGURE 18. *Rapetosaurus krausei* left squamosal (FMNH PR 2189) in **A**, lateral view with dorsal end up, anterior to left; and **B**, medial view with dorsal end up, anterior to right. Scale bar equals 1 cm. **Abbreviations:** p, parietal facet; po, postorbital facet; popr, paroccipital process; q, quadrate facet; stf, supratemporal fenestra.

dial surface is concave. Medially, the proximal end of the ventral process bears a deep quadrate cotylus that cupped the dorsal and lateral sides of the proximal quadrate. On the medial surface, the cotylus is separated from the posterior margin of the indented supratemporal fenestra by a sharp ridge that extends down the anterior margin of the ventral process. Immediately posterior to this ridge, extending the entire length of the ventral process, is a narrow, rugose scar for the lateral plate of the quadrate. Sutural scars on the ventrolateral quadrate indicate that the quadratojugal and squamosal meet in *Rapetosaurus*. The squamosal and quadratojugal do not meet in *Nemegtosaurus* (ZPAL MgD-I/9; Nowinski, 1971), *Diplodocus* (e.g., CM 11161; Holland, 1924), or *Antarctosaurus* (MACN 6804; Huxene, 1929), but do meet in *Brachiosaurus* (e.g., HMN t1, s66, s116; Janensch, 1935/1936) and *Camarasaurus* (e.g., CM 11338; Madsen et al., 1995). The quadratojugal and squamosal of *Quaesitosaurus* (PIN 3906/2; Kurzanov and Bannikov, 1983) are too poorly preserved for this determination. The quadratojugal articulation with the quadrate in each of these taxa is via a single, linear scar, while in *Rapetosaurus* the sutural scar is V-shaped.

Braincase

Exoccipital-Opisthotic—(UA 8698, FMNH PR 2184, FMNH PR 2192; Figs. 2, 19, 25) Two complete exoccipital-opisthotics were recovered from MAD 93-18. One (FMNH PR 2184) articulates perfectly with the associated laterosphenoid, supraoccipital, and basioccipital-basisphenoid from the 1995 quarry level. The second exoccipital-opisthotic (FMNH PR 2192) was found in the lower 1999 quarry level. It is identical in morphology, but smaller than FMNH PR 2184. An additional, poorly preserved partial exoccipital-opisthotic was recovered with the holotype (UA 8698).

The exoccipital and opisthotic are firmly fused to each other, with only a slight trace of a suture in the juvenile elements. The opisthotic forms the anteromedial face of the element above the metotic fissure. The robust exoccipital forms the extreme posteroventral wall of the braincase and the entire lateral border of the foramen magnum. It also has a small con-

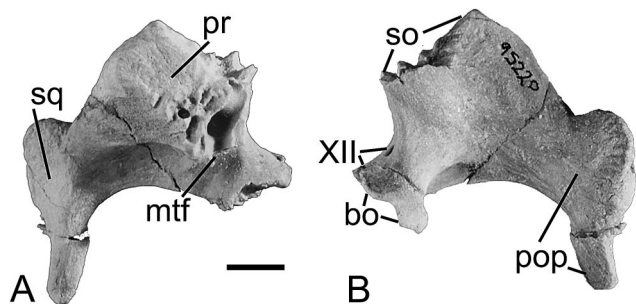


FIGURE 19. *Rapetosaurus krausei* right exoccipital-opisthotic (FMNH PR 2184) in **A**, anteromedial and **B**, posterior views. Scale bar equals 1 cm.

tribution to the occipital condyle, forming its dorsolateral margin.

The robust exoccipital is expanded anteroposteriorly and bears a deeply rugose ventral articulation for contact with the basioccipital. Several small foramina exit the rear of the cranial cavity through the exoccipital. These foramina indicate the path of the hypoglossal nerve (CN XII) roots that enter the exoccipital, join within the body of the exoccipital, and exit laterally behind the paroccipital process via a single foramen. The metotic fissure marks the exits of the glossopharyngeal (CN IX), vagus (CN X), and spinal accessory nerves (CN XI), as well as the jugular vein from the cranial cavity.

Above the metotic fissure, the opisthotic bears two distinctive, anterior, sutural scars for articulation with the prootic (not preserved). The medial of the two sutures is tall, subrectangular, deeply rugose, and intersects the sutural surface for the supraoccipital at a right angle. The lower portion of this articular surface bears an opening for the posterior semicircular canal. Immediately ventral to this suture is the posterior portion of a moderately large inner ear cavity that is connected to the semicircular canals. The posterior half of a foramen that connects the inner ear and metotic fissure is also preserved. The sutural surface for the prootic is bounded laterally and ventrally by a dorsoventrally oriented bony ridge. Fine striae, oriented parallel to this bounding ridge, crease the surface of this sutural area (Fig. 19A).

The dorsomedial surface of the exoccipital-opisthotic is broad and deeply rugose where it meets the supraoccipital above the cranial cavity. In medial view this sutural surface tapers dorsally. The edge of the posterior semicircular canal in the opisthotic is exposed along the anterior margin of this sutural surface. The dorsal margin of the exoccipital is thick and slightly convex along its medial portion. This convex surface bears a transversely oriented facet for articulation with the underside of the parietal.

In posterior view, the anteroposteriorly compressed paroccipital process projects ventrolaterally from the foramen magnum. The paroccipital process has a distinct constriction along its dorsal margin just proximal to its articulation with the squamosal. The constricted portion has a smooth, rounded dorsal margin, separates the squamosal articulation (laterally) from the parietal articulation (medially), and presumably forms the ventral border of a large posttemporal foramen. This dorsal constriction of the paroccipital process results in an extremely convex, nearly hemispherical squamosal articulation in posterior view. The surface of the squamosal articulation is rounded and slightly rugose. Distal to the squamosal articulation, the paroccipital process tapers sharply to a long, thin process that curves distinctly anteroventrally.

Elongate, downturned, and anteroventrally-oriented, non-ar-

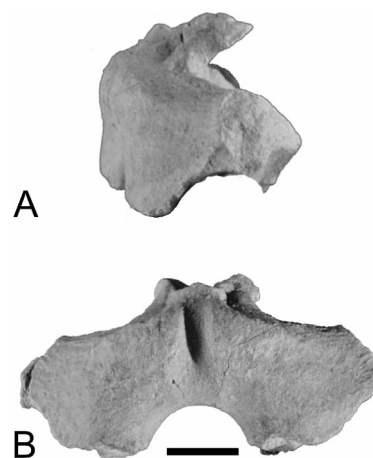


FIGURE 20. *Rapetosaurus krausei* supraoccipital (FMNH PR 2184) in **A**, right lateral view with anterior to right; and **B**, posterior view. Scale bar equals 1 cm.

ticular paroccipital processes have been hypothesized as a potential titanosaur synapomorphy (e.g., Powell, 1986, 1992; Salgado and Calvo, 1997; Wilson and Sereno, 1998). While *Rapetosaurus* shares this general morphology with several other members of Titanosauria, it also sheds light on variation among more specific aspects of titanosaur paroccipital process morphology. A few taxa (e.g., *Quaesitosaurus*, PIN 3906/2) follow the more standard macronarian morphology of short, straight paroccipital processes. Alternatively, the paroccipital processes of *Antarctosaurus* have been reconstructed in a more diplodocoid-like manner, and paroccipital processes are slightly ventrally expanded and terminate in tongue-like distal tips. Personal observations of *Antarctosaurus* (MACN 6804) reveal that paroccipital processes in this taxon are not preserved. A comparison of *Rapetosaurus* with other titanosaurs indicates that most are distinctly characterized by elongate, narrow, paroccipital processes with robust, recurved distal ends. *Rapetosaurus*, *Quaesitosaurus* (PIN 3906/2; Kurzanov and Bannikov, 1983), *Saltasaurus* (PVL 4017/161; Powell, 1992), and *Jainosaurus septentrionalis* (GSI K27/467; Huene and Matley, 1932; ISI R199; Berman and Jain, 1983) share a posterodorsal, paramedial notch in their paroccipital processes that gives a broad exposure to the parietal crest in these taxa.

Supraoccipital—(FMNH PR 2184; Figs. 2, 20, 21, 25) The supraoccipital is a midline element that forms the entire dorsal margin of the foramen magnum and roofs the rear of the cranial cavity. It is axially compressed and robust.

Three distinct but intersecting sutural areas are present on the supraoccipital. First, the ventrolateral supraoccipital bears a thick, rugose, interdigitating sutural surface for the exoccipital. On the anterolateral surface of the supraoccipital, intersecting the exoccipital suture vertically, is a tall, subtriangular facet for the prootic. Intersecting both these subvertical surfaces at approximately 90° is a third, slightly rugose surface on the dorsolateral corner of the supraoccipital. This surface articulates with the underside of the parietal and is confluent with the parietal articular surface on the exoccipital.

The posterodorsal surface of the supraoccipital bears a median groove that is flanked on either side by a parasagittal ridge. A broad-based, forked process extends anteriorly on the midline. Each fork is short and dorsoventrally compressed. A small fossa occurs on the dorsal surface of this forked process, and continues anteriorly across the medial half of each fork. This fossa is separated from the midline groove by a small prominence and likely received a process from the overlying parietal.

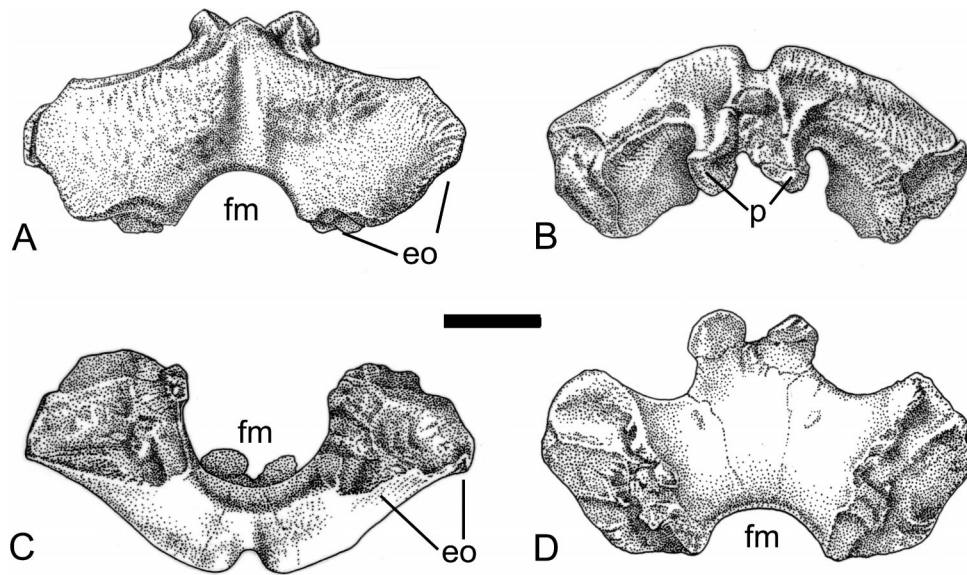


FIGURE 21. *Rapetosaurus krausei* supraoccipital (FMNH PR 2184) in **A**, posterior view; **B**, dorsal view with anterior end down; **C**, anterior view; and **D**, ventral view with anterior end up. Scale bar equals 1 cm. **Abbreviations:** eo, exoccipital facet; fm, foramen magnum; p, parietal facet.

In dorsal view, the thick anterior margin of the supraoccipital is embayed and smoothly rounded lateral to the midline process.

Formation of the nuchal crest in most titanosaurs is via a single midline prominence, as in other neosauropods. *Rapetosaurus*, Titanosauria indet. from Jabalpur (ISI R-162; Chatterjee and Rudra, 1996) and Baja Santa Rosa (MACN RH821), and *Antarctosaurus* (MACN 6804; Huene, 1929) are distinct in the formation of the nuchal crest from two parasagittal prominences separated by a midline depression.

Laterosphenoid-Orbitosphenoid—(FMNH PR 2184; Figs. 22, 25) The laterosphenoid and orbitosphenoid are fused in most sauropods early in ontogeny (Berman and McIntosh, 1978; Madsen et al., 1995), as is the case in *Rapetosaurus*. The laterosphenoid-orbitosphenoid is a flat, winglike element that,

when articulated with the basicranium, leans outward at approximately 45° from vertical (Fig. 25). The lateral surface of the laterosphenoid-orbitosphenoid is relatively flat and smooth. It preserves portions of three large foramina on its ventral margin (CN II, the anterior border of CN V, and a foramen for transmission of the interorbital [or pituitary] vein White, 1958). The laterosphenoid-orbitosphenoid completely encloses two small foramina (CN III, CN IV; Fig. 22).

An elongate, digitate suture for articulation with the frontal extends across the entire dorsal margin of the laterosphenoid-orbitosphenoid. A robust, shelf-like process extends dorsomedially from the posterior corner of the dorsal margin. Its upper surface bears a deeply striated articular surface for the underside of the posterior frontal and the anterior parietal. The smooth ventral surface of this dorsomedial shelf roofs the braincase and forms a ridge-like crista antotica that continues ventrally along the posterior margin of the laterosphenoid-orbitosphenoid. The lateral surface of the dorsomedial shelf is also expanded and likely contacted the underside of the postorbital. In posterior view the laterosphenoid-orbitosphenoid is dominated by a large, triangular facet that extends medially across virtually the entire posterior surface of the dorsomedial shelf. This facet narrows ventrally and has a concave, smooth surface that abuts with the prootic. Immediately below this facet is a smooth, embayed margin that likely represents the anterior edge of a relatively large foramen transmitting the trigeminal nerve (CN V). Thus the trigeminal nerve also pierced the body of the prootic.

The anteroposteriorly constricted ventral margin of the laterosphenoid-orbitosphenoid is dominated by two foramina and two distinct, pillar-like processes that expand ventrally into denticulate articular surfaces to meet the anterior basisphenoid. The tall, narrow dorsal half of a foramen leading into the pituitary fossa indents the ventral margin between these pillars. This opening is slightly restricted along its ventral limit, defining the dorsal portion of this hourglass-shaped foramen. It likely transmitted the interorbital (pituitary) vein (White, 1958; Fig. 22). The ventral portion of this foramen is preserved in the basisphenoid. The large, rounded posterior and dorsal margin of the optic nerve foramen (CN II) lies immediately in front of the

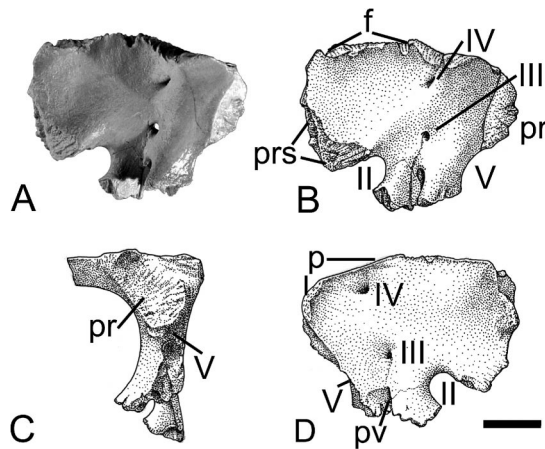


FIGURE 22. *Rapetosaurus krausei* right laterosphenoid-orbitosphenoid (FMNH PR 2184) in **A**, medial view; **B**, lateral view; **C**, posterior view; and **D**, ventral view. Scale bar equals 1 cm. **Abbreviations:** f, frontal facet; p, parietal facet; pr, prootic facet; prs, presphenoid facet; pv, foramen for pituitary vein; I, foramen for cranial nerve I; II, foramen for cranial nerve II; III, foramen for cranial nerve III; IV, foramen for cranial nerve IV; V, foramen for cranial nerve V.

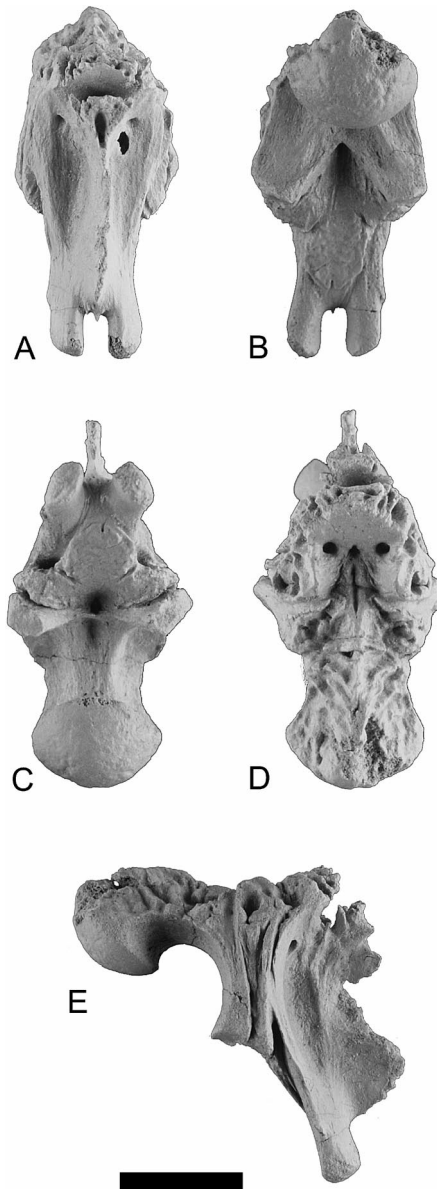


FIGURE 23. *Rapetosaurus krausei* basicranium (FMNH PR 2197) in **A**, anterior view; **B**, posterior view; **C**, ventral view, anterior at top; **D**, dorsal view, anterior at top; and **E**, right lateral view. Scale bar equals 2 cm.

anterior pillar and deeply indents the margin of the orbitosphenoid. Two cranial nerves exit the body of the laterosphenoid-orbitosphenoid. The small, oval foramen for the oculomotor nerve (CN III) exits the braincase posterolaterally approximately 0.5 cm above the foramen for CN V. Slightly posterior to and 1 cm above the oculomotor foramen, a smaller foramen for the trochlear nerve (CN IV) indicates posterodorsal exit through the laterosphenoid-orbitosphenoid. The suture line between the laterosphenoid and orbitosphenoid can be seen on the medial and lateral surface of the fused elements, running between the oculomotor and pituitary foramina. This suture line continues dorsally from the foramen for the oculomotor nerve approximately 0.3 cm.

The anterior margin of the laterosphenoid-orbitosphenoid is dominated by a transversely expanded, triangular facet that narrows dorsally. The rugose articular surface of this facet is sub-

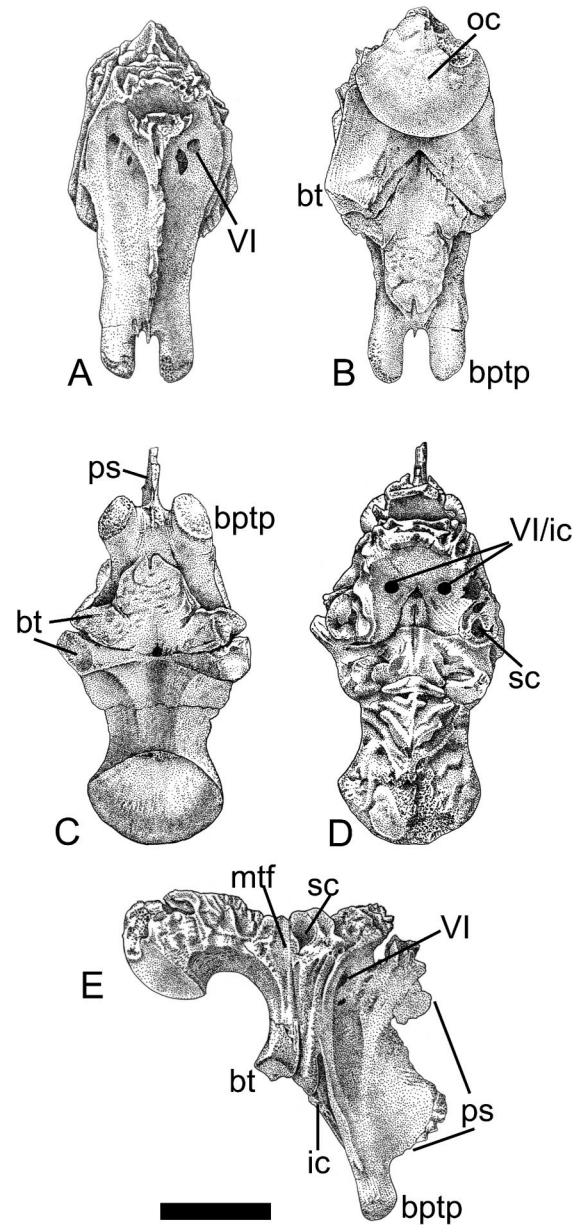


FIGURE 24. *Rapetosaurus krausei* basicranium (FMNH PR 2197) in **A**, anterior view; **B**, posterior view; **C**, ventral view, anterior at top; **D**, dorsal view, anterior at top; and **E**, right lateral view. Scale bar equals 2 cm. **Abbreviations:** **bptp**, basiptyergoid process; **bt**, basal tubera; **ic**, foramen for internal carotid artery; **mtf**, metotic fissure; **oc**, occipital condyle; **ps**, parasphenoid; **sc**, semicircular canals; **VI**, foramen for cranial nerve VI.

parallel to that of the presphenoid articular face on the anterior pillar. When the laterosphenoid-orbitosphenoid is articulated with the basicranium, these two facets face medially and nearly reach the midline. Thus the presphenoid appears to complete both of the optic nerve foramina, as well as forming the median floor of the olfactory nerve exit (CN I). Dorsal to the presphenoid facet, the margin of the laterosphenoid-orbitosphenoid is irregular (and slightly eroded) and oriented dorsolaterally to wall the exit for the olfactory nerve (CN I).

Basicranium—(FMNH PR 2197; Figs. 2, 23, 24, 25) The basicranium consists of fused basioccipital, basisphenoid, and parasphenoid, which form the floor of the braincase. The ba-



FIGURE 25. *Rapetosaurus krausei* articulated supraoccipital, exoccipital-opisthotic, basioccipital, basisphenoid and laterosphenoid (FMNH PR 2184, 2197) in right lateral view. Scale bar equals 2 cm.

sioccipital forms most of the hemispherical occipital condyle. The dorsal surface of the basioccipital narrowly participates in the floor of the posterior cranial cavity, forming a shallow trough for passage of the spinal cord. At least in the juvenile skull, the basioccipital's contribution to the cranial floor is reduced anteriorly until it appears that the basioccipital is either eliminated or severely constrained by contact or near contact of the two exoccipitals. Broad, deeply rugose articular surfaces for the left and right exoccipital-opisthotics (posteriorly) and prootics (anteriorly) slope ventrolaterally at an angle of about 45° to the horizontal along the entire dorsal surface of the basioccipital.

The articular surface of the occipital condyle is well separated from the basal tubera by a moderately long, dorsally arching neck. In lateral view, the condyle is inclined 45° posteroventrally relative to the long axis of the basioccipital tubera. The basioccipital forms the posterior half of the short and robust basal tubera. The basal tubera diverge from one another at an angle of 30–35°. A low ridge extends down the posterior surface of each tuber from the ventral surface of the neck of the condyle. A shallow fossa dimples the surface of the basioccipital where the tubera join.

The basisphenoid is firmly fused to the basioccipital, although traces of their suture remain. The otic region dominates the dorsolateral surface of the basicranium at its junction with the basioccipital. Just anterior to the basioccipital is the metotic fissure, which creases the basioccipital and runs down the side of the element toward the basal tubera. Anterior to the metotic fissure is the otic capsule. Surrounding the otic capsule and immediately anterior to it, the dorsolateral edge of the basisphenoid is deeply rugose to receive the prootic. This suture runs anteroposteriorly.

The basisphenoid forms a broad portion of the cranial floor between and anterior to the otic region. A pair of small, round foramina for the abducens nerve (CN VI) pierces the floor of the basisphenoid on either side of the midline. They pass ventrolaterally through the basisphenoid to exit above the basiptyergoid processes. A small, deep pit occurs on the midline of the endocranial floor between the exits for the abducens nerve. The floor of the cranial cavity terminates anteriorly at the transverse ridge of the dorsum sellae, which forms the posterior

border of the large circular opening of the sella turcica (pituitary fossa). A deeply rugose suture line runs across the anterior margin of the basisphenoid (facing anteriorly), and the anterolateral margin of that element (facing dorsolaterally). The anterolaterally-facing portion of this suture line articulates perfectly with a facet on the posterior pillar of the laterosphenoid-orbitosphenoid. Anterior to this facet on the basisphenoid is a deep, narrow embayment that is continuous with the foramen for the pituitary vein on the laterosphenoid-orbitosphenoid. This foramen opens into the sidewall of the pituitary fossa. Anterior to this foramen is a second, anteriorly facing facet that lies below the pituitary fossa at the anterior margin of the basisphenoid. This facet articulated with the presphenoid (missing).

The basisphenoid forms the anterior half of the robust basal tubera. The distal ends of the tubera are rugose, particularly on their basisphenoid portion. This irregular, slightly rugose surface extends ventrally on the midline down the posterior face of the basiptyergoid processes and may represent an extension of the muscle attachment surface seen on the basal tubera. A small foramen pierces the basicranium between the basal tubera. A small, shallow channel exits this foramen and divides as it courses ventrally across the rugose surface between the basal tubera. Each channel then runs ventrolaterally around the base of the basal tubera to join the deep channel for the internal carotid artery developed in the basisphenoid anterior to the basal tubera. It appears that this small foramen interposed between the basioccipital and basisphenoid may have transmitted arterial blood into the basicranium.

The basiptyergoid processes are conjoined for most of their length, and separate only at their distal extremities. The long basiptyergoid processes of *Rapetosaurus* are more than twice the length of the basal tubera. Their U-shaped separation is marked by the termination of a thin, caudally positioned sheet of the basisphenoid. The distal ends of these processes are gently rounded, slightly rugose, and canted ventrolaterally to meet the pterygoids.

The internal carotid artery entered the basicranium through a moderately large foramen located on the lateral side of the basisphenoid, between the basal tubera and basiptyergoid process. Internally, this canal courses through the basisphenoid to enter the posteroventral aspect of the pituitary fossa. Most of the posterior portion of the pituitary fossa is surrounded by the basisphenoid.

The parasphenoid is completely fused with the basisphenoid, and sutures are not visible. The parasphenoid is represented by a narrow, midline blade of bone that articulates below the pituitary fossa. It is broken anteriorly in FMNH PR 2197 and no parasphenoid rostrum (cultriform process) is preserved.

The orientation and morphology of the basioccipital tubera and the basiptyergoid processes of the basisphenoid are among the most diagnostic of titanosaur features. In *Saltasaurus* (PVL 4017/161; Powell, 1992), basal tubera are nearly planar, and have no significant posterior relief. The tubera arise slightly ventral to the occipital condyle, and the short basiptyergoid processes diverge just ventral to the tubera in a broad, U-shaped division. In contrast, Titanosauria indet. from Jabalpur (ISI R-162; Chatterjee and Rudra, 1996), *Nemegtosaurus* (ZPAL MgD-I/9; Nowinski, 1971), *Malawisaurus* (SMU MAL-202; Gomani, 1998), and *Rapetosaurus* all exhibit basal tubera that have great posterior relief and are quite expansive. The basal tubera in these taxa diverge well below the ventral margin of the occipital condyle. The basiptyergoid processes diverge even more ventrally in these taxa, giving the basiptyergoid region of the basisphenoid an extremely elongate morphology. Basiptyergoid processes among these taxa also diverge at variable locations and patterns. In some taxa, such as *Antarctosaurus wichmannianus* (MACN 6804; Huene, 1929), Titanosauria indet. from Jabalpur (ISI R-162; Chatterjee and Rudra, 1996), and



FIGURE 26. *Rapetosaurus krausei* pterygoids. **A**, FMNH PR 2191 left pterygoid in medial view, anterior to right; **B**, UA 8698 right pterygoid in medial view, anterior to left; and **C**, UA 8698 left pterygoid in medial view, anterior to right. Scale bar equals 3 cm.

Nemegtosaurus (ZPAL MgD-I/9; Nowinski, 1971), basiptyergoid processes divide proximally via a deep V-shaped notch, with lengthy processes. In *Quaesitosaurus* (PIN 3906/2; Kurzanov and Bannikov, 1983) the posterior face of the basal tubera is planar, and basiptyergoids diverge just ventral to the basal tubera, and are characterized by a short, robust basiptyergoid processes that exhibit a narrow, U-shaped division. In *Rapetosaurus*, basiptyergoids diverge distally, resulting in an extensive and elongate basisphenoid, but relatively short basiptyergoid processes. This division is via a narrowed U-shaped notch similar to that of *Quaesitosaurus* (PIN 3906/2), instead of the deep “V” of other taxa. Finally, basiptyergoid processes in *Saltasaurus* (PVL 4017/161; Powell, 1992) and *Rapetosaurus* project anterolaterally. Other titanosaurs have ventrolaterally-directed basiptyergoid processes (e.g., Titanosauria indet. from Jabalpur ISI R-162; Chatterjee and Rudra, 1996), while still others have posterolaterally-oriented processes (e.g., *Quaesitosaurus*, PIN3906/2). In contrast to *Brachiosaurus* (e.g., HMN t1, s66, s116; Janensch, 1935/1936) and *Camarasaurus* (e.g., CM 11338; Madsen et al., 1995) which have poorly developed, posteriorly flat basal tubera and a horizontally oriented occipital condyle, the *Rapetosaurus* basicranium bears several general similarities to diplodocoids, including the anteroventral orientation of the occipital condyle, and anteriorly oriented basal tubera and basiptyergoid processes.

Palate

Pterygoid—(UA 8698, FMNH PR 2191; Figs. 2, 26, 27) Both juvenile (FMNH PR 2191) and holotype (UA 8698) pterygoids are preserved. No other palatal bones have been recovered. The pterygoid is a nearly flat, triradiate element with a sub-vertical orientation. Three distinct processes radiate from the pterygoid body: an anterodorsal wing for contact with the contralateral pterygoid, an anteroventral ectopterygoid wing, and a posterior quadrate wing.

The anterodorsal pterygoid wing is the longest of the three processes. The width of this process increases only slightly at its distal extreme, and its medial surface bears a large oval facet for a broad, abutting contact with the contralateral pterygoid. This facet extends nearly the full height of the pterygoid’s an-

teroventral process but does not reach the distal end of the process. At the anterior base of this wing, a small but distinctive lateral depression marks the contact of the palatine with the pterygoid.

The anteroventral ectopterygoid wing is long and slender, and forms an angle of about 90° with the pterygoid wing. It narrows distally, and terminates in two distinct articular facets. The larger, ventral facet faces anteromedially; the small dorsal facet faces anterodorsally. Presumably, both these facets articulated with the ectopterygoid (not preserved).

The posterodorsal quadrate wing meets the pterygoid wing at an angle of about 90°. It extends posterodorsally, widening until its lateral surface contacts the medial surface of the pterygoid wing of the quadrate. This contact involves the entire distal end of the quadrate wing of the pterygoid. The medial surface of the quadrate wing bears a large shallow facet for the reception of the basiptyergoid process of the basisphenoid. Unlike many other sauropods (e.g., *Camarasaurus*, CM 11338; Madsen et al., 1995; *Dicraeosaurus*, HMN dd519; Janensch, 1935/1936), this fossa lacks a distinct posterodorsally-oriented “hook,” and instead is merely a shallow fossa for the basiptyergoid process of the basisphenoid.

Pterygoids have only been described for three titanosaurs: *Nemegtosaurus* (ZPAL MgD-I/9; Nowinski, 1971), *Quaesitosaurus* (PIN 3906/2; Kurzanov and Bannikov, 1983), and *Rapetosaurus*. All three share platelike pterygoids, with processes that radiate in the same plane. This is in stark contrast to the complex, three-dimensional pterygoids of other sauropod taxa (e.g., *Brachiosaurus*, HMN t1, s66, s116; Janensch, 1935/1936; *Camarasaurus*, CM 11338; Madsen et al., 1995; *Dicraeosaurus*, HMN dd519; Janensch, 1935/1936; *Diplodocus*, CM 11161; Berman and McIntosh, 1978). *Nemegtosaurus* (ZPAL MgD-I/9; Nowinski, 1971) and *Rapetosaurus* share the general morphology of the pterygoid wing with a broad and extensive facet for articulation with the opposite element. *Rapetosaurus* pterygoids meet at an angle of about 45°, in contrast to the 25° convergence in *Nemegtosaurus* (ZPAL MgD-I/9; Nowinski, 1971). Similarly, although *Rapetosaurus*, *Nemegtosaurus* (ZPAL MgD-I/9), *Quaesitosaurus* (PIN 3906/2; Kurzanov and Bannikov, 1983), and *Brachiosaurus* (HMN t1; Janensch, 1935/

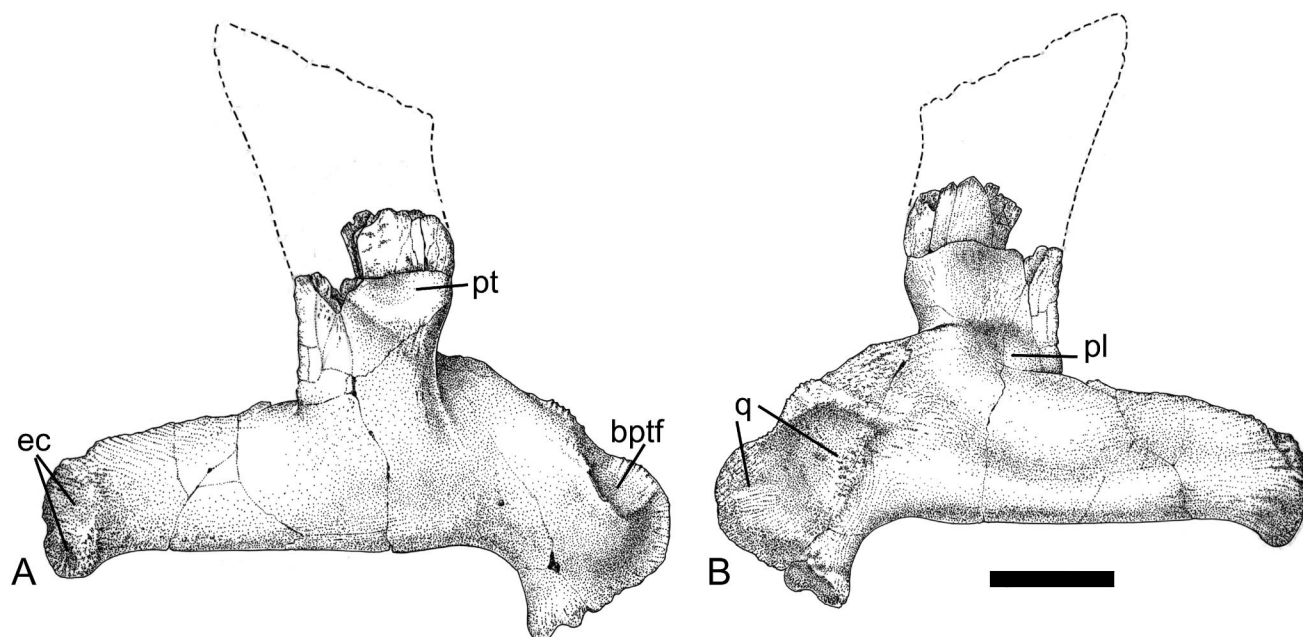


FIGURE 27. *Rapetosaurus krausei* left pterygoid reversed (UA 8698) in **A**, medial view, anterior to left; and **B**, lateral view with anterior to right. Pterygoid wing is reconstructed based on right pterygoid UA 8698, which preserves the complete flange. Scale bar equals 3 cm. **Abbreviations:** **bptf**, basipterygoid fossa; **ec**, ectopterygoid process; **pl**, palatine process; **pt**, pterygoid process; **q**, quadrate process.

1936) share the absence of a pterygoid hook, the basipterygoid process articulation greatly varies among these taxa. In *Brachiosaurus*, the basipterygoid processes articulate on a medially directed shelf. In contrast, the posterodorsal process in *Rapetosaurus* is only slightly concave. Among sauropods, *Rapetosaurus*, *Quaesitosaurus* (PIN 3906/2), and *Nemegtosaurus* (ZPAL MgD-I/9) uniquely share the shallow depression for the reception of the basipterygoid processes.

Lower Jaw

The holotype (UA 8698) includes the dentary and several postdentary elements. An isolated juvenile surangular (FMNH PR 2187) and angular (FMNH PR 2194) are also referred to *Rapetosaurus*.

Dentary—(UA 8698; Figs. 28, 29) The left dentary is lightly built with 11 alveoli in its anterior half; six unerupted teeth are preserved. Articulated dentaries form a U-shaped symphysis, with each dentary curving gently towards the anterior midline. The curvature of the dentary toward the midline begins at the level of its minimum vertical depth (at approximately the 4th or 5th alveolus). The dorsoventral axis of the vertical symphyseal surface is nearly perpendicular to the long axis of the dentary, and is triangular in medial view with a narrow ventral apex and broad dorsal base. The dentary is slightly dorsoventrally expanded anteriorly, but damage to this ventral margin makes it impossible to determine the full extent of this expansion. The dentary and postdentary elements provide an estimated lower jaw length of 39 cm. Postdentary bones extend only 9 cm posterior to the dentary. Based on the associated lower jaw elements, the adult *Rapetosaurus* skull is estimated at approximately 40 cm in length.

In lateral view, the dentary is marked by distinct neurovascular foramina positioned below each alveolus. Posterior to the fifth alveolus the dentary gradually deepens to its posterior end. The posterior portion of the dentary is divided into distinct dorsal and ventral rami, immediately behind the last (11th) alveolus. The dorsal ramus bears a deep, elongate facet on its lateral side for reception of the surangular. In medial view, a fossa is developed along the ventral margin of the dorsal ramus and the dorsal margin of the anterior ventral ramus. It continues forward as a V-shaped impression across the body of the dentary to the level of the seventh alveolus and was presumably covered by the splenial. The splenial likely continued nearly to the symphysis, as indicated by the well-defined Meckelian groove, but probably did not contribute to the mandibular symphysis (as in *Brachiosaurus*, HMN s66, s116; Janensch, 1935/1936). The

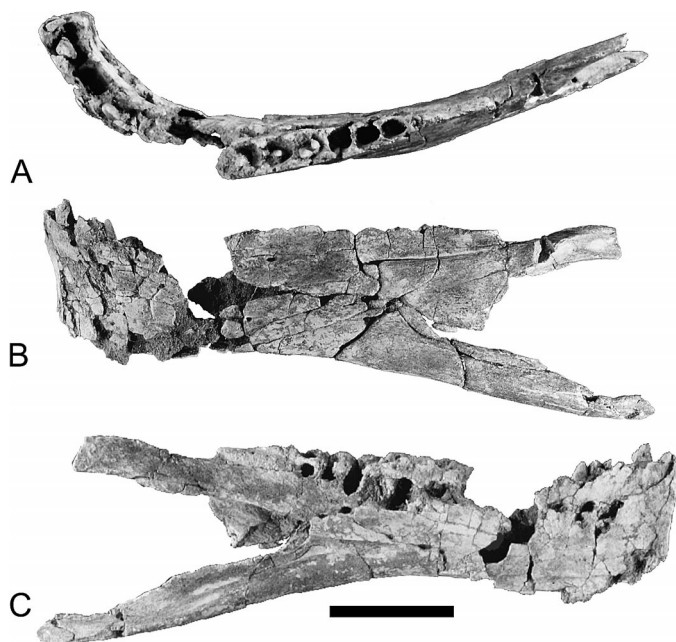


FIGURE 28. *Rapetosaurus krausei* left dentary (UA 8698) in **A**, dorsal view, anterior to left; **B**, lateral view; and **C**, medial view. Scale bar equals 5 cm.

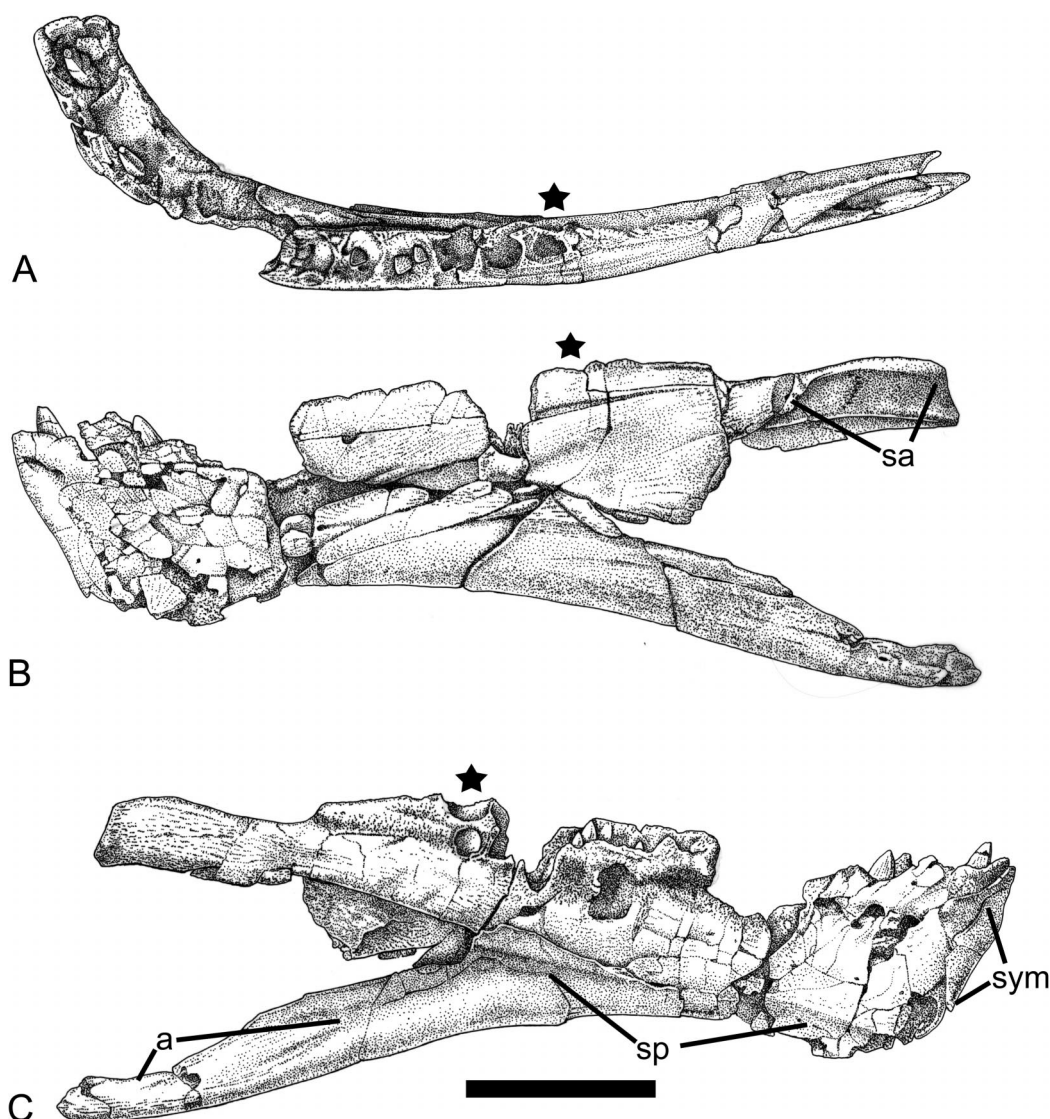


FIGURE 29. *Rapetosaurus krausei* left dentary (UA 8698) in **A**, dorsal view, anterior to left; **B**, lateral view; and **C**, medial view. Star marks the last (11th) alveolus. Scale bar equals 5 cm. **Abbreviations:** a, angular facet; sa, surangular facet; sp, splenial facet; sym, mandibular symphysis.

distal end of the dorsal ramus is broken, but appears to have tapered to a narrow terminus. The ventral ramus is long and tapered. It bears a slightly concave facet on its entire dorso-medial surface that receives the anterior portion of the angular. The ventral margin of most of the dentary and the ventral ramus is broadly rounded. The deep posterior emargination formed by the diverging rami is covered laterally by the large surangular.

The alveoli in the dentary decrease in size posteriorly and are bound fused interdental plates (the medial plate). The medial plate is perforated by 11 large, round neurovascular foramina; one opening is associated with the base of each alveolus. The medial plate above the foramina is composed of fused interdental plates, and is consistently lower than the lateral plate. Posterior to the last alveolus, a short, rugose ridge of bone (~3.5 cm) supplements the oral margin, ending abruptly at the base of the dorsal ramus. *Rapetosaurus*, *Nemegtosaurus* (ZPAL MgD-I/9; Nowinski, 1971), *Quaesitosaurus* (PIN 3906/2; Kurzanov and Bannikov, 1983), *Camarasaurus* (e.g., CM 11338; Madsen et al., 1995), and *Brachiosaurus* (e.g., HMN s66, s116; Janensch, 1935/1936) have robust dentaries that are dorsoventrally expanded posteriorly and anteriorly. When compared to

Rapetosaurus, *Malawisaurus* (SMU MAL 174; Jacobs et al., 1993) has a relatively shallow dentary without significant posterior expansion. Comparison of the dentary of *Rapetosaurus* with that of the titanosaurs *Ampelosaurus* MD-E C3-336), *Nemegtosaurus* (ZPAL MgD-I/9), and *Quaesitosaurus* (PIN 3906/2; Kurzanov and Bannikov, 1983) reveals overall similarities in (1) the number of teeth, (2) the position of teeth, and (3) the orientation of the mandibular symphysis. In each of these taxa (as well as in *Brachiosaurus* and *Camarasaurus*), minimum tooth counts range from 9 (*Ampelosaurus* MD-E C3-336; Le Loueff, 1995) to 15 (*Malawisaurus*, Jacobs et al., 1993). All of these taxa exhibit a gently curving dentary that meets in a broad, U-shaped symphyseal region. Similarly, in all but *Nemegtosaurus* (ZPAL MgD-I/9), alveoli are present along 60–80% of the dorsal margin of the dentary. The restriction of the alveoli to the anterior 2/3 of the dentary also distinguishes *Rapetosaurus* and other titanosaurs from diplodocoid taxa in which the tooth row is restricted to the anterior one-third of the dentary.

Surangular—(UA 8698, FMNH PR 2187; Figs. 2, 30) The surangular is a deep, elongate, oval plate that covers most of

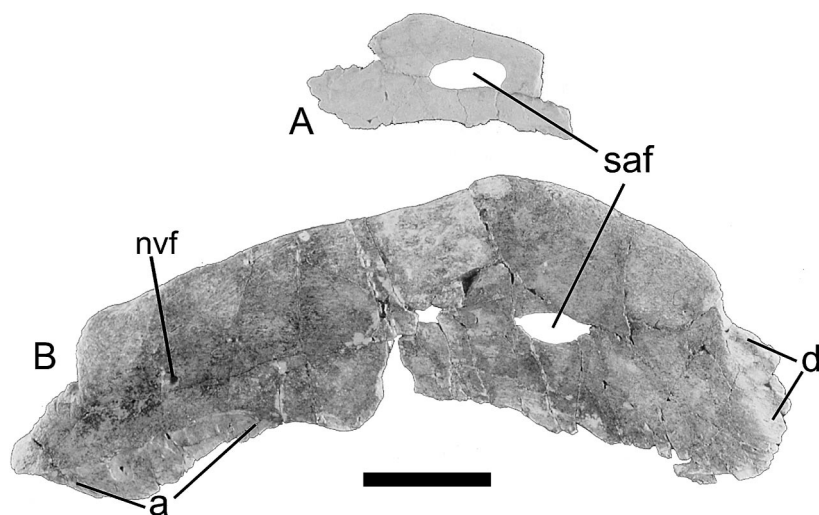


FIGURE 30. *Rapetosaurus krausei* right surangulars in lateral view. **A**, FMNH PR 2187; **B**, UA 8698. Scale bar equals 3 cm. **Abbreviations:** **a**, angular facet; **d**, dentary facet; **nvf**, neurovascular foramen; **saf**, surangular foramen.

the post-alveolar region of the mandible in lateral view. The ventral margin of this element is concave and slightly damaged in both specimens. The thick dorsal margin is convex. Its apex occurs at the thickened coronoid eminence in the proximal one-third of the element, similar to *Brachiosaurus* (e.g., HMN s116; Janensch, 1935/1936) and *Camarasaurus* (e.g., CM 11338; Madsen et al., 1995). A moderately large, oval surangular foramen pierces the body of the element anteroventral to the prominent coronoid elevation in the holotype. This foramen is centered between the dorsal and ventral margins. The foramen is centered slightly behind the coronoid elevation in the juvenile specimen. Since these elements are otherwise identical, these differences may reflect their contrasting ontogenetic stages. Interestingly, the absolute size and morphology of the foramen appears to be maintained through ontogeny; in both specimens it is anteroposteriorly elongate and approximately the same width. The medial surface of the coronoid elevation of the surangular bears a facet for the distal end of the dorsal ramus of the dentary. On the lateral surface of the anterior surangular, an anterodorsal facet is overlapped by the dentary at the point where its rami diverge.

Posterior to the coronoid eminence, the surangular thickens as it narrows somewhat dorsoventrally. A large, deep facet is developed on its ventrolateral surface for reception of the posterior half of the angular. A moderately large neurovascular foramen opens above this facet on the lateral surface of the surangular. The posterodorsal margin of the surangular is deeply notched and slightly rugose. A shallow oval depression for reception of the prearticular is positioned medially. The *Rapetosaurus* surangular has a broad lateral exposure similar to that of *Brachiosaurus* (HMN s116), *Camarasaurus* (CM 11338), *Nemegtosaurus* (ZPAL MgD-I/9), and *Quaesitosaurus* (PIN 3906/2; Kurzanov and Bannikov, 1983), but unlike that of diplodocoid taxa (e.g., *Diplodocus*, CM 11161).

Angular—(UA 8698 FMNH PR 2194; Fig. 31) The long angular tapers anteriorly and exhibits a smooth, sigmoidal curvature in lateral view. The angular is nearly as long as the dentary and forms most of the posterior half of the ventral margin of the lower jaw. The ventral margin of the angular is thick and rounded, but thins to a narrow dorsal margin. Anteriorly, the ventrolateral margin of the angular bears a deep fossa for reception of the ventral ramus of the posterior dentary. The

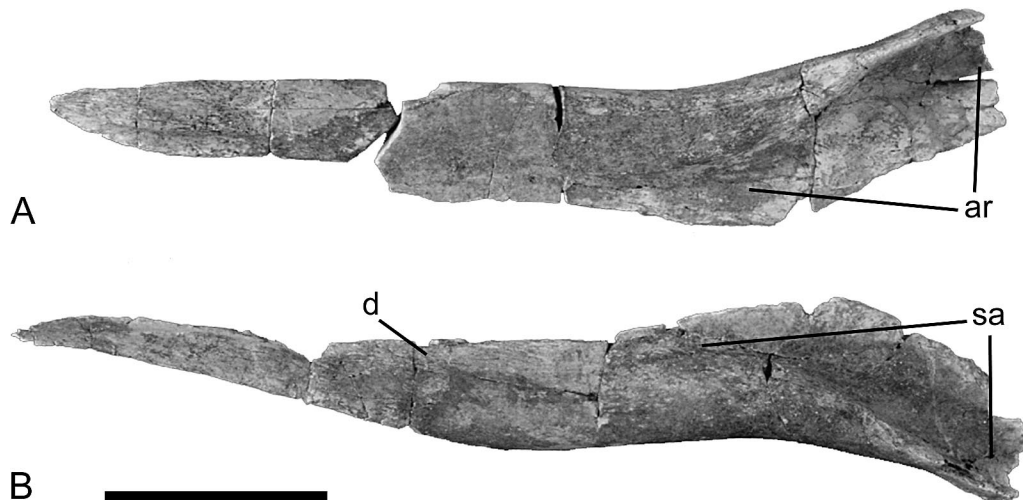


FIGURE 31. *Rapetosaurus krausei* left angular (UA 8698) in **A**, dorsal view, anterior to left; and **B**, lateral view, anterior to left. Scale bar equals 5 cm. **Abbreviations:** **ar**, articular facet; **d**, dentary facet; **sa**, surangular facet.



FIGURE 32. *Rapetosaurus krausei* maxillary tooth (UA 8698). **A**, worn tooth in lingual view showing high-angled wear facet and **B**, unworn maxillary tooth in mesial/distal view. Scale bar equals 1 cm. **Abbreviations:** wf, wear facet.

anterior angular thus sits in an elongate groove located along the dorsomedial edge of the ventral ramus of the dentary. Posterior to this facet, the angular curves ventrally and flares slightly dorsally. The posterior margin of the angular is deeply scalloped and slightly rugose. In medial view, a large depression extends across the entire dorsal margin, deepening posteriorly until it covers the entire surface of the angular. The ventral margin of the posteriormost angular wraps medially to floor this depression, while the dorsolateral extension laterally overlaps the surangular. Presumably, the articular then rested on the angular, across the deep, ventral portion of the depressed region of the angular. It may have also extended upward to meet the posteroventral margin of the surangular.

Dentition

Teeth—(UA 8698, FMNH PR 2196; Fig. 32) A total of eight teeth were recovered with the maxilla, 11 teeth were contained in the dentary, and five additional loose teeth were found associated with UA 8698. Three teeth have also been recovered from MAD 93–18 (FMNH PR 2196). The teeth are buccolingually expanded and slightly elliptical in cross-section. Worn isolated teeth from the juvenile specimen, as well as worn teeth associated with the adult bear flat, lingually oriented and highly angled wear facets, whereas unerupted teeth terminate in tapered tips with slight mesiodistal carina. Unworn teeth in the maxilla and dentary also demonstrate that tooth crowns are not greatly expanded relative to the roots, as in some other sauropods (e.g., *Brachiosaurus*, HMN t1, s66, s116; Janensch, 1935/1936; *Camarasaurus*, CM 11338; Madsen et al., 1995; Wilson and Sereno, 1998; *Malawisaurus*, SMU MAL 6, 174; Jacobs et al., 1993). The teeth of *Rapetosaurus* are moderately large and

robust, contrasting with the narrower, “pencil-like” teeth of diplodocoids. *Rapetosaurus* teeth are generally similar to the teeth of *Nemegtosaurus* (ZPAL MgD-I/9; Nowinski, 1971; Barrett, 2000) and *Quaesitosaurus* (PIN 3906/2; Kurzanov and Bannikov, 1983) in diameter and overall shape. However, instead of the lingually oriented, high-angled facets of *Rapetosaurus*, *Nemegtosaurus* bears mesial and distal wear facets (Nowinski, 1971). Mesial and distal tooth wear facets have also been observed in *Brachiosaurus* (e.g., HMN t1, s66, s116) and *Camarasaurus* (e.g., CM 11338). Tooth Slenderness Indices (length of crown divided by maximum mesiodistal width; Upchurch, 1998) in *Rapetosaurus* exceed 5.0, a ratio also observed in other titanosaurs (including *Ampelosaurus*, MDE C3–336; Loeuff, 1995; *Malawisaurus*, SMU MAL-6, 174; Jacobs et al., 1993; *Nemegtosaurus*, ZPAL MgD-I/9; Nowinski, 1971; *Quaesitosaurus*, PIN 3906/2). Barrett (2000) provided a summary of tooth function in *Rapetosaurus* based on SEM analysis of tooth wear facets. He concluded that the microwear on *Rapetosaurus* teeth included coarse scratches parallel to the long axis of the crown and randomly distributed pits. The pattern may have been caused by durable food particles or grit crushed between teeth upon occlusion (Wilson and Sereno, 1998; Barrett, 2000).

SUMMARY AND CONCLUSION

Holotype and referred *Rapetosaurus* cranial material is among the most complete and best preserved of any described titanosaur, and yields interesting new insights into overall titanosaur skull morphology. The skull of *Rapetosaurus* is similar to diplodocoids in its overall shape, with retracted external nares and an elongated snout. However, tooth distribution throughout the upper and lower jaws, and the articulations of bones comprising the margins of the external narial region and orbit are more similar to those of macronarians like *Camarasaurus* and *Brachiosaurus*. The maxilla, basicranium, paroccipital process, and pterygoid are among the most diagnostic elements of the *Rapetosaurus* skull, along with the enlarged antorbital fenestra, the anteroventrally oriented braincase, and the mandible. Due to the dearth of cranial data for other known titanosaurs, this new Malagasy sauropod has great potential to clarify higher and lower level titanosaur phylogeny. In light of the *Rapetosaurus* crania described herein, it is apparent that there may not be a narrowly constrained bauplan for the skull of titanosaurs and that generalizations about evolution based on the previously known and fragmentary fossil data require re-evaluation.

ACKNOWLEDGMENTS

We would like to thank R. Rogers, D. Krause, S. Sampson, M. Carrano, D. Chure, and J. Wilson for their many comments and advice during the preparation of this paper. V. Alifanov, S. Apestegia, S. Bandyopadhyay, J. Bonaparte, M. Borsuk-Bialynicka, T. Fiorillo, E. Gomani, L. Salgado, and D. Unwin allowed access to specimens. M. Hallett provided the cranial reconstruction in Figure 1, and J. Martinez provided technical illustrations of individual elements. M. Stewart and T. Ready took the photographs. Funding was provided by the National Science Foundation, the National Geographic Society, the Jurassic Foundation, the Geological Society of America, and the Gabor Inke Graduate Student Fellowship.

LITERATURE CITED

- Barrett, P. 2000. The evolution of sauropod feeding mechanisms; pp. 79–122 in H. D. Sues (ed.), *Evolution of Herbivory in Terrestrial Vertebrates*. Cambridge University Press, Cambridge.
- Berman, D. S., and S. L. Jain. 1983. The braincase of a small sauropod dinosaur (Reptilia: Saurischia) from the Upper Cretaceous Lameta

- Group, Central India, with a review of Lameta Group Localities. *Annals of the Carnegie Museum* 51:405–422.
- Berman, D. S., and J. S. McIntosh. 1978. Skull and relationships of the Upper Jurassic sauropod *Apatosaurus* (Reptilia, Saurischia). *Bulletin of the Carnegie Museum of Natural History* 8:1–35.
- Bonaparte, J. F., and R. Coria. 1993. Un nuevo y gigantesco sauropodo titanosaurio de la Formacion Rio Limay (Albiano-Cenomanio) del a Provincia del Neuquen, Argentina. *Ameghiniana* 30:271–282.
- Boule, M. 1896. Note preliminaire sur les debris de Dinosauriens envoyes au museum par M. Bastard. *Bulletin du Museum d'Histoire Naturelle de Paris* II:347–351.
- Chatterjee, S., and D. K. Rudra. 1996. KT events in India: impact, rifting, volcanism and dinosaur extinction. *Memoirs of the Queensland Museum* 39:489–532.
- Curry, K. A. 2001. The evolutionary history of the Titanosauria. Ph.D. dissertation, State University of New York at Stony Brook, Stony Brook, 552 pp.
- Curry, K. A., and C. A. Forster. 1999. New evidence of titanosaurian sauropods in the Late Cretaceous of Madagascar. Abstracts, VII International Symposium on Mesozoic Terrestrial Ecosystems. Buenos Aires, p. 20.
- Curry, K. A., and C. A. Forster. 1999. New sauropods from Madagascar: a glimpse into titanosaur cranial morphology and evolution. *Journal of Vertebrate Paleontology* 19(3, Supplement):40A.
- Curry Rogers, K. 2001a. The anatomy and phylogeny of a new titanosaurid from Madagascar (Upper Cretaceous Maevarano Formation). XVII Jornadas Argentinas de Paleontologia de Vertebrados, p. 8.
- Curry Rogers, K. 2001b. A new sauropod from Madagascar: implications for lower level titanosaur phylogeny. *Journal of Vertebrate Paleontology* 21(3, Supplement):43A.
- Curry Rogers, K. 2002. Titanosaur tails tell two tales: a second Malagasy titanosaur with saltosaurid affinities. *Journal of Vertebrate Paleontology* 22(3, Supplement):47–48A.
- Curry Rogers, K., and C. A. Forster. 2001. The last of the dinosaur titans: a new sauropod from Madagascar. *Nature* 412:530–534.
- Depéret, C. 1896a. Note sur les Dinosauriens Sauropodes et Théropodes dans le Crétacé supérieur de Madagascar. *Bulletin de la Société Géologique de France* 21:176–194.
- Depéret, C. 1896b. Sur l'existence de Dinosauriens, Sauropodes et Théropodes dans le Crétacé supérieur de Madagascar. *Comptes Rendus Hebdomadaires des Séances de l'Académie des Sciences (Paris)* 122:483–485.
- Gomani, E. 1998. Sauropod cranial elements from Malawi: implications of titanosaurid cranial morphology. *Journal of Vertebrate Paleontology* 18(3, Supplement):46A.
- Holland, W. J. 1924. The skull of *Diplodocus*: *Memoirs of the Carnegie Museum* 9:379–403.
- Huene, F. v. 1929. Los Saurisquios y Ornithisquios del Cretaceo Argentino. *Anales del Museo La Plata* 2:1–196.
- Huene, F. v., and Matley, ?. 1932. The Cretaceous Saurischia and Ornithischia of the central provinces of India. *Memoirs of the Geological Survey of India* 21:1–74.
- Jacobs, L. L., D. A. Winkler, W. R. Downs, and E. M. Gomani. 1993. New material of an Early Cretaceous titanosaurid sauropod dinosaur from Malawi. *Palaeontology* 36:523–534.
- Janensch, W. 1935/1936. Di Schädel der Sauropoden *Brachiosaurus*, *Barosaurus* und *Dicraeosaurus* aus den Tendaguruschichten Deutsch-Ostfrikas. *Palaeontographica (Suppl.7)* 2:147–298.
- Krause, D. W., J. H. Hartman, and N. A. Wells. 1997. Late Cretaceous vertebrates from Madagascar: implications for biotic change in deep time; pp. 3–43 in S. D. Goodman and B. D. Patterson (eds.), *Natural change and human impact in Madagascar*. Smithsonian Institution, Washington, D. C.
- Krause, D. W., R. R. Rogers, C. A. Forster, J. H. Hartman, G. A. Buckley, and S. D. Sampson. 1999. The Late Cretaceous vertebrate fauna of Madagascar: implications for Gondwanan paleobiogeography. *GSA Today* 9:1–7.
- Kurzanov, S. M., and A. F. Bannikov. 1983. A new sauropod from the Upper Cretaceous of Mongolia. *Paleontological Journal* 2:90–96.
- Le Loueff, J. 1995. *Ampelosaurus atacis* (nov. gen., nov. sp.), un nouveau Titanosauridae (Dinosauria, Sauropoda) du Cretace superieur de la Haute Vallee de L'Aude (France). *Comptes Rendus de L'Academie des Sciences de Paris (ser. IIa)* 321:693–699.
- Madsen, J. H., Jr., J. S. McIntosh, and D. S. Berman. 1995. Skull and atlas-axis complex of the Upper Jurassic sauropod *Camarasaurus* Cope (Reptilia: Saurischia). *Bulletin of the Carnegie Museum of Natural History* 31:1–115.
- Martinez, R. 1998. An articulated skull and neck of Sauropoda (Dinosauria: Saurischia) from the Upper Cretaceous of Central Patagonia, Argentina. *Journal of Vertebrate Paleontology* 18(3, Supplement): 61A.
- Nowinski, A. 1971. *Nemegtosaurus mongoliensis* n. gen. n. sp. (Sauropoda) from the uppermost Cretaceous of Mongolia. *Palaeontologica Polonica* 25:57–81.
- Powell, J. E. 1986. Revision de los titanosauridos de America del Sur. Ph.D. dissertation, Universidad Nacional de Tucuman, Tucuman, 340 pp.
- Powell, J. E. 1992. Osteologia de *Saltasaurus loricatus* (Sauropoda-Titanosauridae); pp. 166–230 in J. L. Sanz and A. D. Buscalioni (eds.), *Los Dinosaurios y su Entorno Biotico*. Cuenca, Instituto "Juan de Valdes."
- Rogers, R. R., J. H. Hartman, and D. W. Krause. 2000. Stratigraphic analysis of Upper Cretaceous rocks in the Mahajanga Basin, northwestern Madagascar: implications for ancient and modern faunas. *Journal of Geology* 108:275–301.
- Salgado, L., and J. O. Calvo. 1997. Evolution of titanosaurid sauropods. II: the cranial evidence. *Ameghiniana* 34:33–48.
- Salgado, L., J. O. Calvo, and R. A. Coria. 1997. Evolution of the titanosaurid sauropods. I: phylogenetic analysis based on the postcranial evidence. *Ameghiniana* 34:3–32.
- Upchurch, P. 1998. The phylogenetic relationships of sauropod dinosaurs. *Zoological Journal of the Linnean Society* 124:43–103.
- White, T. E. 1958. The braincase of *Camarasaurus lentus* (Marsh). *Journal of Paleontology* 32:477–494.
- Wilson, J. A., and P. C. Sereno. 1998. Early evolution and higher-level phylogeny of sauropod dinosaurs. *Journal of Vertebrate Paleontology* 18(3, Supplement):1–68.
- Wiman, C. 1929. Die Kriede-Dinosaurier aus Shantung. *Paleontologica Sinica (C)* 6:1–67.
- Witmer, L. M. 2001. Nostril positions in dinosaurs and other vertebrates and its significance for nasal function. *Science* 293:850–853.
- Yu, C. 1993. The skull of *Diplodocus* and the phylogeny of the Diplodocidae. Ph.D. dissertation, University of Chicago, Chicago, 150 pp.

Received 18 April 2002; accepted 24 February 2003.